Preprint
UCRL-JC-136490

The MACHO Project Sample of Galactic Bulge High-Amplitude δ Scuti Stars: Pulsation Behavior and Stellar Properties

C. Alcock, R.A. Allsman, D.R. Alves, T.S. Axelrod, A.C. Becker, D.P. Bennett, K.H. Cook, K.C. Freeman, M. Geha, K. Griest, M.J. Lehner, S.L. Marshall, B.J. McNamara, D. Minniti, C. Nelson, B.A. Peterson, P. Popowski, M.R. Pratt, P.J. Quinn, A.W. Rodgers, W. Sutherland, M.R. Templeton, T. Vandehei and D.L. Welch

U.S. Department of Energy

Lawrence Livermore National Laboratory

This article was submitted to
Summit Conference
Seattle, WA
July 29-31, 1999

November 16, 1999

The MACHO Project Sample of Galactic Bulge High-Amplitude δ Scuti Stars: Pulsation Behavior and Stellar Properties

C. Alcock[1,2], R.A. Allsman[3], D. R. Alves[4], T.S. Axelrod[1,5], A.C. Becker[2,6], D.P. Bennett[7], K.H. Cook[1,2], K.C. Freeman[5], M. Geha[1], K. Griest[2,8], M.J. Lehner[9], S.L. Marshall[1], B.J. McNamara[10], D. Minniti[11], C. Nelson[1,12], B.A. Peterson[5], P. Popowski[1], M.R. Pratt[13], P.J. Quinn[14], A.W. Rodgers[5], W. Sutherland[15], M.R. Templeton[10,17,18], T. Vandehei[8], and D.L. Welch[16]

(The MACHO Collaboration)

[1]Lawrence Livermore National Laboratory, Livermore, CA 94550

E-mail: alcock, tsa, kcook, mgeha, stuart, popowski@llnl.gov

[2]Center for Particle Astrophysics, University of California, Berkeley, CA 94720

[3]Supercomputing Facility, Australian National University, Canberra, ACT 0200, Australia

E-mail: Robyn.Allsman@anu.edu.au

[4]Space Telescope Science Institute, 3700 San Martin Dr., Baltimore, MD 21218

E-mail: alves@stsci.edu

[5]Mt Stromlo & Siding Spring Observatories, Australian National Univ., Weston ACT 2611, Australia

E-mail: kcf, peterson, pjq, alex@merlin.anu.edu.au

[6]Department of Astronomy, University of Washington, Seattle, WA 98195

E-mail: stubbs, becker@astro.washington.edu

[7]Physics Department, University of Notre Dame, Notre Dame, IN 46556

E-mail: David.Bennett.27@nd.edu

[8]Department of Physics, University of California, San Diego, CA 92093

E-mail: griest, vandehei@astrophys.ucsd.edu

[9]Department of Physics, University of Sheffield, Sheffield S3 7RH, UK

E-mail: m.lehner@shef.ac.uk

[10]Astronomy Department, New Mexico State University, Box 30001, Dept 4500, Las Cruces, NM 88003

E-mail: bmcnamar, mtemplet@nmsu.edu

[11]Depto. de Astronomia, P. Univ. Catolica, Casilla 104, Santiago 22, Chile

Email: dante@astro.puc.cl

[12]Department of Physics, University of California, Berkeley, CA 94720

[13]Center for Space Research, MIT, Cambridge, MA 02139

Email: mrp@mit.edu

[14]European Southern Observatory, D-85748 Garching bei München, Germany

E-mail: pjq@eso.org

[15]Department of Physics, University of Oxford, Oxford OX1 3RH, U.K.

E-mail: wjs@oxds02.astro.ox.ac.uk

[16]Department of Physics and Astronomy, McMaster University, Hamilton, ON L8S 4M1, Canada

E-mail: welch@physics.mcmaster.ca

[17]Thermonuclear Applications Group, X-Division, MS B220, Los Alamos National Laboratory, Los

Received _____; accepted _____

Alamos, NM 87545

[18]Work towards PhD thesis at New Mexico State University

ABSTRACT

We have detected 90 objects with periods and lightcurve structure similar to those of field δ Scuti stars, using the Massive Compact Halo Object (MACHO) Project database of Galactic bulge photometry. If we assume similar extinction values for all candidates and absolute magnitudes similar to those of other field high-amplitude δ Scuti stars (HADS), the majority of these objects lie in or near the Galactic bulge. At least two of these objects are likely foreground δ Scuti stars, one of which may be an evolved nonradial pulsator, similar to other evolved, disk-population δ Scuti stars. We have analyzed the light curves of these objects and find that they are similar to the light curves of field δ Scuti stars and the δ Scuti stars found by the Optical Gravitational Lens Experiment (OGLE). However, the amplitude distribution of these sources lies between those of low- and high-amplitude δ Scuti stars, which suggests that they may be an intermediate population. We have found nine double-mode HADS with frequency ratios ranging from 0.75 to 0.79, four probable double- and multiple-mode objects, and another four objects with marginal detections of secondary modes. The low frequencies (5-14 cycles d^{-1}) and the observed period ratios of ~ 0.77 suggest that the majority of these objects are evolved stars pulsating in fundamental or first overtone radial modes.

Subject headings: Galaxy: center — stars: blue stragglers — stars: classification — stars: oscillations — stars: variables: delta Scuti

1. Introduction

Pulsating stars have been used for several decades to probe the physical properties of stars, including their masses, luminosities, internal compositions, and structure. Many different types of pulsating stars exist over a broad range of masses, temperatures, and evolution states (for a concise list, see Becker 1998). Most lie off the main sequence, and thus can only be used to study the interiors of objects which have undergone substantial (and occasionally poorly understood) evolution. One exception to this is the class of near main-sequence pulsators known as δ Scuti stars. The δ Scuti stars are A-F stars on the Cepheid instability strip with masses ranging from 1.0 to 3.0 $M_{\odot}$. They are dwarfs or subgiants which have not yet reached the red giant branch, and hence are at most only moderately evolved objects. Pulsation studies of these objects can therefore yield useful information about the internal properties of main sequence stars more massive than the Sun (Breger 1998).

The δ Scuti stars are divided into several subclasses. One division is between stars with Population I and II abundances, namely the δ Scuti (Pop I) and SX Phoenicis (Pop II) stars. The SX Phoenicis stars lie at the low end of the mass range of the δ Scuti stars. Another major division is between the low-amplitude δ Scuti stars (LADS) and high-amplitude δ Scuti stars (HADS) (Rodriguez et al. 1996). LADS are most often on or close to the main sequence, and frequently pulsate in nonradial modes. These stars often have very complex pulsation spectra, which can be used as a probe of their deep interior structure. HADS are most often radial pulsators and are more commonly found off the main sequence, near core hydrogen exhaustion and ignition of the H-burning shell.

In recent years, HADS have not received as much attention as LADS. The pulsations of HADS cannot be used to probe the stellar core, which is important for evolution studies. Furthermore, HADS typically pulsate in a few modes at most, which limits the precision of asteroseismology. However, HADS are now gaining more attention. First, they appear to have a period-luminosity relation making them useful secondary distance indicators (McNamara 1997, Petersen & Høg 1998). Second, their presence in nominally old stellar populations like the halo and globular clusters, and their identification as blue stragglers in many of these populations indicate they may not follow the standard stellar evolution scenario (cf. Sills, Bailyn, & Demarque 1995). Finally, hydrodynamic simulations of δ Scuti stars studying lightcurve structures as functions of envelope composition (Guzik 1992) and radial mode order (Bono et al. 1997 and Templeton, Guzik, and McNamara 1999) show that radial pulsations can provide some structural and compositional information on the envelopes of these objects.

Large-scale photometry projects like MACHO (Alcock et al. 1997) and OGLE (Udalski et al. 1997, and references therein), and targeted observations of globular cluster interiors with HST (Gilliland et al. 1998) have uncovered hundreds of new δ Scuti stars, the majority of which are HADS. With the substantial increase in the numbers of these objects, it is now possible to study their characteristics as a class. In this paper, we present a new sample of δ Scuti stars found by the MACHO Project. In section 2, we discuss the sample selection and time-series analysis of these objects, and present our catalog. In section 3, we discuss the general results of the time series. In section 4, we discuss the details of the pulsation behavior, including lightcurve structure and the doubly- and multiply-periodic objects, with a brief discussion of the physical information that can be obtained from this data.

2. MACHO Data: sample and analysis

The MACHO Project goals and data acquisition have been described elsewhere at length (see Cook et al. 1995 and Alcock et al. 1997) and will only be briefly summarized here. The MACHO data are collected simultaneously in two filters (similar to Kron-Cousins V and R) on two focal planes with the 1.27m Great Melbourne Telescope at Mount Stromlo Observatory in Australia. The MACHO Project images approximately 200 42'x42' fields in the Galactic bulge, the Large and Small Magellanic Clouds (LMC and SMC) during the course of a year, with images of the bulge fields taken approximately once per night during the appropriate observing season. Exposure times for the bulge, LMC and SMC are 150, 300, and 600 seconds, respectively. Photometry of all sources in the images is performed using SoDoPHOT (Alcock et al. 1999), to a limiting magnitude of roughly 20. Light curves of individual point sources within each field are then compiled and are monitored for variations due to gravitational microlensing. Long-term monitoring of these fields has serendipitously yielded detections of many thousands of variable stars in addition to the detections of microlensing events.

2.1. Sample selection

To find δ Scuti stars in the MACHO database, we searched the MACHO database of variable stars in the Galactic bulge. We limited our search to the bulge because δ Scuti stars in the LMC and SMC are too faint to be reliably detected. δ Scuti stars have absolute V-magnitudes of 1 to 2.5, so LMC and SMC δ Scuti stars would have apparent magnitudes of roughly 20. This is too faint to detect variability with amplitudes of ~ 0.5 mag, like those of δ Scuti stars. We selected objects showing variability on timescales of

0.3 to 0.03 days, as determined using "super-smoother" period-fitting programs (Reimann 1994 and Akerlof et al. 1994). δ Scuti stars can have periods in the range of 0.2 to 0.03 days ($\nu = 5 - 35$ cycles d^{-1}) or less (Breger 1979). We note that the shortest-period δ Scuti stars are usually fainter, main-sequence stars, and have the lowest amplitudes, making them difficult to detect in the MACHO database. Therefore, the sample presented here is biased against the high-frequency, low-amplitude pulsators, and we concentrate only on the high-amplitude δ Scuti stars. In principle, we could also select objects with dereddened $(V - R)$ of $\sim 0.2 \pm 0.1$, but reddening in the bulge fields is highly variable, and such a selection procedure would be ill defined. Our period-search criterion yielded a sample of 132 objects from the MACHO bulge fields.

2.2. Data calibration and analysis

Observations were made simultaneously in two broadband filters, similar to but wider than Kron-Cousins V and R. We discarded data points if a detection was not made in both filters, because our classification of these objects depends on the behavior in the two different passbands. This resulted in the removal of approximately 10% of the observations per data set. After removal of non-coincident points, we transformed the instrumental magnitudes, v_i and r_i, to standard V and R magnitudes using the following transformation:

$$V = v_i - 0.18 \cdot (v_i - r_i) + 23.70, \tag{1a}$$

$$R = r_i + 0.18 \cdot (v_i - r_i) + 23.41, \tag{1b}$$

(Alcock et al. 1999). We note that our initial selection of candidates was done using the data and calibrations as of early 1997, and as a consequence, our results are slightly different from those of Minniti et al (1998) and Templeton et al (1998). We discuss these differences in the next section. Prior to our time-series analysis, the observation times are also corrected to heliocentric Julian date.

After calibration and removal of bad points, the average data set contains ~ 450 measurements covering a span of ~ 2100 days between March 1993 and December 1998. The average photometric error per point of the data is 0.05 magnitudes, but there is substantial variation in data quality among our sample objects. At $V \sim 13.5$ the mean error is ~ 0.02 mag, and increases to ~ 0.08 and higher at $V \sim 18$ and fainter. However, the majority of stars in our sample are brighter than $V = 18$, and only 2 sources are fainter than $V = 19$.

2.3. Time-series analysis

Time-series analysis was performed on the V and R data for each object. To compute the spectra, we used the method outlined in Templeton et al. (1997), where we applied a discrete Fourier transform (DFT) to the data, selected the highest peak, prewhitened the data with the resulting sine wave, and repeated the process until no statistically significant signals remained. We note that while the data is highly undersampled in time (by a factor of 10 to 30 below the Nyquist rate), the DFT is still reliable in this case because the data is sampled quasi-randomly in lightcurve phase. This reduces the sidelobe ambiguity which normally results from undersampled data, though it does not eliminate it entirely, as we note below. We show a sample transform and phased light curve of a doubly-periodic star in Figure 1. In our analysis, we do not take into account period changes or binary motion which could have an impact on a DFT analysis. Breger and Pamyatnykh (1998) have shown that δ Scuti stars show period changes of one part in 10^{-6} *at most* and only one object in our sample (discussed in section 4.3) showed evidence of signal modulation due to binarity.

The frequency precision is determined from the following formula

$$\delta\nu = \frac{3\sigma_N}{\sqrt{N}(t_N - t_0)A}, \tag{2}$$

where $\delta\nu$ is the frequency error in cycles d^{-1}, σ_N is the mean scatter of the data in magnitudes after prewhitening, N is the number of data points, $t_N - t_0$ is the total length of the data set in days, and A is the amplitude of the observed pulsation mode. The uncertainty in the phase is determined using the relation

$$\delta\phi = \frac{1}{\sqrt{2P}} \tag{3}$$

where $\delta\phi$ is the phase error in radians, and P is the peak power normalized by the mean power level (see Templeton et al. 1997 and references therein). A signal is considered real if $P > 10$ in either filter, and the signal is clearly visible in the other filter. Frequency errors $\delta\nu$ for the highest-amplitude modes average ~ 0.00005 cycles d^{-1} even with the relatively low S/N. This is because the error term is dominated by $1/(t_N - t_0)$, where $t_N - t_0 \sim 2100$ days. The average phase error $\delta\phi$ is ~ 0.1. In no case is P greater than ~ 280, so $\delta\phi$ is never smaller than ~ 0.04 radians.

All of our 132 objects showed a 1 cycle day^{-1} aliasing in their Fourier transforms due to the data sampling. This aliasing caused some uncertainty in determining the correct frequency for $\sim 15\%$ of the

sample. For the majority of these stars, the main frequency was easily identifiable and prewhitening eliminated that period and it's aliases. In some cases, prewhitening did not completely remove the signal or it's aliases, and these frequency identifications might be uncertain by ± 1 cycle day^{-1}. Fortunately, several of these objects had non-sinusoidal lightcurves and the first Fourier harmonic was used to determine the correct primary pulsation mode. Secondary pulsation modes were *not* used to select the correct sidelobe, since both frequencies could be off by 1 cycle day^{-1} and still yield a reasonable period ratio.

To determine which stars among the 132 candidates are δ Scuti stars, we visually inspected the light curves and measured the ratio of R- and V-band amplitudes. Visual inspection allowed us to clearly distinguish the majority of objects as either δ Scuti stars or W Ursa Majoris contact binaries, because the light curves of each type are usually quite distinctive, and few other types of variable star exist with these short periods (see Sterken & Jaschek 1996). For those sources with noisy, poorly-sampled, or ambiguous light curves, we also used the ratio of R- and V-band amplitudes. For δ Scuti stars, this ratio is less than one, because the effective temperature can change by several hundred Kelvin over the pulsation cycle (Solano & Fernley 1997), while for W Ursa Majoris stars, it is close to one because the two components have nearly equal temperatures. This quantity is also useful because it is a reddening-free parameter, since the amplitudes are not affected by reddening. Using this ratio, we find a mean $A_R/A_V \sim 0.78$ for the δ Scuti stars, and $A_R/A_V \sim 0.93$ for the W Ursa Majoris stars, with a division between the two classes at ~ 0.85. This value is slightly different from the $A_R/A_V \sim 0.8$ used in Minniti et al. (1998), which is primarily due to the coupling of the two filters in the different calibrations.

Based on the above analyses, 90 δ Scuti stars were identified in the original sample of 132 candidates. We present the list of δ Scuti stars and their pulsation properties in Table 1. Detailed ephemerides including frequencies, amplitudes and phases for each δ Scuti star are given in Table 2.

3. Observational properties and period-amplitude distribution

The majority of objects in the MACHO sample of Galactic bulge δ Scuti stars have pulsation behavior similar to field HADS. Seventy of the 90 δ Scuti stars in the bulge fields have V-amplitudes higher than 0.1 mag, and none are below 0.04 mag. Even our lowest-amplitude objects have amplitudes which are still higher than those of field LADS. The lack of extremely low amplitude (1-10 millimag) objects is most likely due to the S/N of the MACHO photometry. The discrete Fourier transform can detect signals at the 0.3σ-level with a 99% confidence level (cf Mullan, Herr, Bhattacharyya 1992). The mean photometric

error per point of the MACHO data is of order 0.05 magnitudes, so ideally, stars with amplitudes in the 0.015-0.02 magnitude range could be detectable in the MACHO database. However, we only found one object with very low amplitude pulsations, and it appears to be a foreground object. Ultimately, the severe temporal undersampling and low S/N relative to the pulsation amplitudes make objects like field LADS difficult to detect in the bulge. Therefore, we cannot make any conclusions on the existence of LADS in the Galactic bulge at the present time.

Figure 2 compares the amplitude distribution of the MACHO δ Scuti stars to the Rodriguez et al. (1994) sample of known field δ Scuti stars. The vast majority of known field δ Scuti stars have amplitudes less than 0.05 magnitudes, so the MACHO δ Scuti stars are more like the field HADS. However, we note that the amplitude distribution of the MACHO δ Scuti stars lies between that of the field HADS (centered at ~ 0.28 mag) and LADS (< 0.1 mag). We speculate that the MACHO stars may be a distinct population that is physically different from both the field HADS (of which many are SX Phoenicis variables) and field LADS.

Another clue to the physical properties of these sources is the distribution of their amplitudes versus apparent magnitude. Figure 3 shows the distribution of V-amplitudes versus *apparent* V magnitudes. Objects with amplitudes less than 0.1 mag appear to be smoothly distributed in apparent magnitude, indicating they may be a mix of foreground disk objects and bulge stars, but the lack of any objects with amplitudes significantly higher than 0.1 and brighter than $V \sim 16.5$ is striking. We suggest that most if not all of the stars with $V > 16$ are within the Galactic bulge.

There is some evidence the MACHO objects may not have formed as normal, isolated stars. The MACHO color-magnitude diagram of Baade's window overlaid with the MACHO δ Scuti stars is shown in Figure 4. The δ Scuti stars are slightly blueward and more luminous than the main-sequence turn-off for the majority of bulge stars. This suggests that these objects may be like the blue stragglers observed in other cluster populations, and might provide an answer as to why these early-type stars are found in a nominally old stellar population. Observations of δ Scuti blue stragglers in globular clusters (cf. Gilliland et al. 1998) suggest that δ Scuti stars are present even in very old stellar populations, and that they may form due to stellar collisions or mass transfer in binary systems. There is even some evidence of field δ Scuti stars undergoing similar processes, for example the multiply-periodic LADS θ Tucanae (DeMey, Daems, & Sterken 1998, and Templeton, Bradley, & Guzik 1999). However, some studies of stellar populations in the Galactic bulge (cf. Holtzman et al. 1998, Ng et al. 1996, and Holtzman et al. 1993) indicate the presence of multiple populations of stars, some of which may have formed within the past 1-2 Gyr. Therefore,

a definitive statement on the age and properties of these objects cannot be made based *solely* on their location on the color-magnitude diagram. We will discuss pulsational indicators of the physical properties of *individual* objects briefly in the next section, but we leave a detailed theoretical analysis of their properties for a later paper.

4. Pulsation behavior

In this section, the pulsation behavior of the MACHO δ Scuti stars is discussed. Section 4.1 discusses the observed light curve structures of these objects, section 4.2 describes the confirmed doubly- and multiply-periodic stars, section 4.3 describes the suspected doubly- and multiply-periodic stars, and section 4.4 summarizes the pulsational behavior and discusses stellar characteristics that can be derived from this study.

4.1. Light curve structure

The δ Scuti stars in the MACHO database show a variety of pulsation behaviors, though the majority are large amplitude pulsators, and none have short (< 0.07 d) periods common among main-sequence LADS. Seventy-six of the 90 stars in our sample show clear non-sinusoidal variations indicated by the presence of the second (or higher order) Fourier harmonics. We list the pulsation parameters A_{N1} and ϕ_{N1} for these 76 objects in Tables 3a and 3b, and plot them in Figures 5a and 5b. A_{N1} is the ratio of the N-th to first (fundamental) Fourier harmonic amplitude and ϕ_{N1} is the phase difference of the N-th and first Fourier harmonic, defined by

$$\phi_{N1} = \phi_N - N \cdot \phi_1 \tag{4}$$

(Simon & Lee 1981, Morgan, Simet, & Bargenquast 1998).

A_{21} ranged from 0.1 to 0.5 in V-band for these sources. A_{21} is not correlated with period (see Figures 5a and 5b), but it is correlated with the pulsation amplitude A_1 (see Figure 6). The higher amplitude objects have higher A_{21} values. This is most likely a property of the stars rather than an observational selection effect; if our ability to detect A_{21} were limited by the S/N this would more severely impact the low-amplitude pulsators. Since we find low-A_{21} objects among the low-amplitude pulsators, this cannot

be an observational bias. Therefore, the high-amplitude pulsators apparently cannot be sinusoidal. One possible explanation for this is that as the star is driven to higher amplitudes (and hence higher radial velocity variations), shocks in the envelope may perturb the lightcurve at specific stages of the pulsation cycle. A modeling program using hydrodynamic simulations to study the high amplitude behavior of these stars is in preparation (Templeton 1999).

Unlike the amplitude ratios, the phase differences are nearly constant for the Fourier series, and show no correlation with either period or amplitude. In V-band, the phase differences (Figure 5) show only moderate scatter ($\pm 0.5 - 1$ radian) around a constant value. This result is quite different from that seen for Cepheids (Simon & Lee 1981), and might be related to the narrower range of periods and physical sizes seen in δ Scuti stars. The average phase differences and scatter for the MACHO sample are nearly identical to those of Morgan, Simet, & Bargenquast (1998) in their study of the OGLE δ Scuti/SX Phoenicis stars. However, a significant difference exists between MACHO and OGLE stars for the parameter ϕ_{31}. Unlike the OGLE sample, no MACHO stars have $\phi_{31} \sim 4$. Morgan, Simet, and Bargenquast (1998) suggest the OGLE stars with ϕ_{31} that are well separated from the main clump at ~ 2 radians may be SX Phoenicis stars. Therefore, it could be possible that no SX Phe (Population II) stars are found among the MACHO δ Scuti stars, but the physical explanation for the light curve behavior is not yet clear. We also note Antonello et al. (1986) found a trend of phase differences with period in 24 field HADS. It is not clear why the bulge HADS do not exhibit a similar trend, although the stars listed by Antonello et al. have higher light amplitudes, and may be physically different. This is discussed further in section 4.4.

4.2. Confirmed double- and multiple-mode pulsators

At least 10 and as many as 18 δ Scuti stars in our sample pulsate in two or more modes. The ten objects listed in Table 4a are those with clearly identified secondary modes. Two of these stars - MACHO 109.20634.24 and 109.20638.40 - are probably foreground sources given their observed magnitudes and colors (see Table 1). MACHO 109.20634.24 is probably an evolved nonradial pulsator, while MACHO 109.20638.40 (along with MACHO 104.20389.1202) has an anomalously low period ratio. In this section, we discuss each of the ten best candidates.

4.2.1. MACHO 109.20634.24

MACHO 109.20634.24 has a mean V-magnitude of 13.71. If we assume a maximum luminosity of 30 $L_\odot$, this star cannot be further than ~ 3.5 kpc, and is thus not a member of the bulge population. This star is pulsating in four simultaneous modes with frequencies of 5.61, 5.47, 6.93, and 6.86 cycles d^{-1}, indicating that it is a nonradial pulsator. These four frequencies were detected both with the shorter 1993-1996 data set and with the longer 1993-1998 data set. Therefore, we are confident that all of these frequencies are real. This star may be useful for asteroseismology, since it appears at least two of these modes are nonradial ones, and nonradial pulsations propagate deeper into the star than do radial pulsations. However, a precise asteroseismological analysis is difficult with few pulsation modes, so additional, high-precision photometry is needed for a secure model fit. We also note that the low frequencies of these modes probably indicate this is an evolved star, and core degeneracy will make seismology difficult as with δ Scuti itself (Templeton et al. 1997).

4.2.2. MACHO 104.20389.1202 and 109.20638.40

MACHO 104.20389.1202 and 109.20638.40 are double-mode pulsators, with mean V-magnitudes of 18.28 and 14.31 respectively. Using the same argument as for 109.20634.24, MACHO 109.20638.40 is likely a foreground star. These two stars have anomalously low frequency ratios of 0.7507 and 0.7510, respectively. Double-mode, radially pulsating δ Scuti stars have frequency ratios not much less than 0.77 for fundamental and first overtone pulsation, with higher $n/(n+1)$ combinations having higher ratios. We analyzed both the 1993-1996 and 1993-1998 data sets for both of these objects and detected the same frequencies in both cases. Therefore, we believe the modes are real and the stated frequencies are correct. There are three possible explanations for these frequencies. First, the objects could be misidentified RR Lyrae pulsators. We consider this to be very unlikely given the high pulsation frequencies relative to those of most RR Lyrae stars. Second, one or both of the observed modes in these stars could be nonradial. This is also unlikely, because if the modes were nonradial, we would not expect to see similar frequency ratios in two different stars. Finally, the stars could be highly evolved and metal rich. Petersen & Christensen-Dalsgaard (1996) and Templeton (1999) computed fundamental-to-first overtone frequency ratios for stars of different abundances, and found a progression toward lower ratios in stars with higher metal abundances and older ages. A star with $Z \geq 0.02$ could have a fundamental frequency and frequency ratio in this range, if it were very old and cool (< 6800 K).

4.2.3. MACHO 114.19840.890, 114.19969.980, 119.19574.1169, 128.21542.753, and 162.25343.874

These five objects are all double-mode δ Scuti stars, with frequency ratios ranging from 0.7708 to 0.7742, indicating that they are pulsating in the fundamental and first overtone radial modes. Their mean V-magnitudes range from 17.79 to 18.60, placing them within the Galactic bulge. Their ν_0 frequencies range from 7.964 to 9.683 cycles d^{-1}, which is also reasonable for fundamental mode δ Scuti stars. The spread in frequency and in period ratio indicates that these five do not form a homogeneous group of objects, and that they must have different ages and masses or both. Overall, their frequencies suggest that they are not close to the red edge of the instability strip, but the fact that they are pulsating in fundamental mode indicates that they must be evolved.

We note that MACHO 128.21542.753 has a first overtone mode which is stronger than the fundamental. This may indicate it is further from the red edge than the others. Therefore, caution must be used when applying a period-luminosity relation to these objects. For example, the period-luminosity relation given in Petersen & Høg (1998) would yield a 0.4 magnitude difference in absolute magnitude depending on the frequency used. Therefore, a clear mode identification should be made before applying a period-luminosity relation to these objects.

4.2.4. MACHO 114.20368.797 and 121.22427.551

MACHO 114.20368.797 and 121.22427.551 are double-mode stars with frequency ratios of 0.7903 and 0.7830 respectively. The frequency ratio of 0.7903 for MACHO 114.20368.797 is too high for fundamental and first overtone pulsation, so it is either second and first overtone pulsation, or one or both modes is nonradial. The ratio of 0.7830 for MACHO 121.22427.551 is reasonable for a less-evolved fundamental and first overtone pulsator (Petersen & Christensen-Dalsgaard 1996). If both of these objects are radial pulsators, then they must be younger than the bulk of the other double-mode δ Scuti stars in the MACHO sample, which again indicates the heterogeneity of the MACHO δ Scuti stars.

4.3. Possible double- and multiple-mode candidates

The remaining eight candidates in Table 4b have marginally detected frequencies or peculiar pulsation spectra. Of these eight stars, three appear to be double mode, radial pulsators, but the secondary pulsation modes are near the detection limit and may not be real signals. Three more stars clearly appear to have

secondary modes, and are listed as tentative identifications because of their weak tertiary modes. One star may have a variable frequency due to binary motion or period changes. Finally, one star is almost certainly a double mode star, but the secondary frequency is not clearly detected due to 1 cycle per day aliasing.

4.3.1. Weak double-mode candidates

Three of the δ Scuti stars, MACHO 114.20108.1218, 115.22573.263, and 116.24384.481, appear to be double-mode, radial fundamental-first overtone pulsators, with period ratios of 0.78690, 0.77241, and 0.77271 respectively. However, the secondary modes are very weak, and lie near the signal detection limit. Follow-up photometry with higher S/N will be required to confirm these frequencies.

4.3.2. Multiple-mode candidates

Three of the δ Scuti stars, MACHO 109.20378.2701, 119.19835.439, and 162.25475.771, may be pulsating in non-radial modes. MACHO 109.20378.2701 had two closely-spaced modes at 9.6384 and 9.6556 cycles d^{-1} detected using the 1993-1996 data set. The 1993-1998 data set yields a third weak frequency at 10.1348 cycles d^{-1}. Such close frequency spacing (0.017 cycles d^{-1} or 0.2 μHz, for the two strongest modes) is uncommon in δ Scuti stars, but could be explained by rotational splitting. If this mode is nonradial, then the true frequency may be split into a multiplet by the rotation of the star, according to the formula

$$\delta\nu = \pm m \cdot (1 - C_{\ell k}) \cdot \Omega \tag{5}$$

where $\delta\nu$ is the frequency split, (k, ℓ, m) are the spherical harmonic indices of the mode, C is the splitting constant, and Ω is the rotation speed of the star (Unno et al. 1989). Since only three modes are visible, it would be impossible to fit a theoretical model to these modes, so none of these parameters can be determined without additional data. These modes may also be of two different ℓ-values with close frequencies, and one mode may be excited by the other. Again, a clear determination of this cannot be made without additional modes present. However, the close spacing of the pulsation modes indicates non-radial pulsation modes, making this star an interesting candidate for follow-up observations.

MACHO 119.19835.439 and 162.25475.771 appear to be double-mode pulsators, but have a tertiary mode immediately adjacent to the overtone. As with MACHO 109.20378.2701, the frequency spacing is

extremely small; $\delta\nu$ is 0.055 cycles d^{-1} (0.65 μHz) for 119.19835.439 and 0.08 cycles d^{-1} (0.93 μHz) for 162.25475.771. This behavior is also seen in the prototype of the class, δ Scuti (Templeton et al. 1997). That star has two modes at 8.33 and 8.57 cycles d^{-1}, and one or both of them may be non-radial modes caused by resonant excitation by the (undetected) second overtone. The same phenomenon may be occurring in these objects.

4.3.3. Double-mode candidate with sidelobe confusion

MACHO 120.21785.976 appears to be a double mode star, but it has a very low frequency ratio of 0.7120. This is much lower than what would be expected for a radially pulsating δ Scuti star. However, if the observed secondary mode is shifted by one cycle d^{-1} to 11.982 cycles d^{-1}, the resulting frequency ratio of $\sim$ 0.771 is typical of that found in double-mode δ Scuti stars in this frequency range. Further observations are needed to obtain a more secure frequency determination for this star.

4.3.4. Phase problem or period change?

Finally, there is one star, MACHO 162.25996.475, which could not be properly phased. Prewhitening of the light curve with the main pulsation frequency of 10.80128 cycles d^{-1} yielded a second frequency at 10.80047 cycles d^{-1} with very high power. This suggests either some form of modulation with a timescale of 3.38 years (0.00081 cycles d^{-1}) or possible a change in frequency of the main pulsation mode. A change in the pulsation frequency would be particularly interesting, and the rate of change ($\Delta\Pi/\Pi \sim 4 \cdot 10^{-8}$) is reasonable compared to those seen in other δ Scuti stars (Breger & Pamyatnykh 1998). Again, further observations may be useful for better determining the pulsation behavior of this object.

4.4. Summary of pulsation behavior

The advanced evolution state of the MACHO δ Scuti stars is indicated by the low pulsation frequencies (5 - 15 cycles d^{-1}) and the high light amplitudes (0.05 mag and higher). Furthermore, the frequency ratios of $\sim$ 0.77 seen in the confirmed double mode stars indicate that they are pulsating primarily in the fundamental and first overtone modes, suggesting that these stars must lie nearer the red edge of the instability strip. Overall, the MACHO δ Scuti stars resemble evolved field HADS, though as we mentioned both in section 3 and in section 4.1, their amplitudes and phase differences show some differences from their

field counterparts. The lack of a trend of phase difference with frequency in the MACHO and OGLE bulge δ Scuti stars is curious when compared to field HADS. As we mentioned in section 4.1, the field HADS studied by Antonello et al. (1986) have average light amplitudes higher by a factor of two than the MACHO stars. Our sample is also slightly different because it lacks stars with very low frequencies (4 - 5 cycles d^{-1}) or high frequencies (15 - 20 cycles d^{-1}). A possible explanation for this is that the narrower range of periods of our sample masks the trends in amplitudes and phase differences seen in field HADS. We consider this likely because the trend in the field HADS is rather small - only 1.2 radians over the range of 4 to 20 cycles d^{-1}, and our phase errors range from 0.04 to 0.2 radians per star. However, the lack of *any* significant trend in ϕ_{21} is interesting, and may indicate real physical differences between the field and bulge δ Scuti stars.

We also briefly address the location of these objects in the instability strip. As mentioned above, the frequency ratios near 0.77 indicate fundamental-first overtone pulsation, and since the pulsation frequencies of the double-mode stars are not significantly different from the other stars in our sample, we suspect that the MACHO δ Scuti stars are primarily fundamental or low-overtone (first or second) pulsators. One of the goals of this project is to assess whether we can use *light curve structure* as an indicator of overtone. As mentioned in the introduction, Bono et al. (1997) and Templeton, Guzik, & McNamara (1999) have used *theoretical* models to suggest that overtone pulsators have more non-sinusoidal lightcurves than do fundamental pulsators. The fact that we see a broad range of A_{21} and no trend of A_{21} with period, coupled with the presence of fundamental-first overtone pulsators with median A_{21} values argues against this. Possible reasons for the contradictory results may be the impact of convection in the stellar envelope, a non-standard evolution history, or peculiar envelope abundances. More work along these lines is clearly warranted and is currently underway (Templeton 1999). In particular, non-standard evolution and composition differences compared to field HADS may be important because these objects are most likely blue stragglers as mentioned in section 3. Several hydrodynamic calculations of stellar collisions have been made in recent years. The results of Sills, Bailyn, & Demarque (1995) and Rasio (1996) show that blue stragglers must be fully mixed by some process during or after the collision of the progenitor stars. If blue stragglers form in this manner, it would have a very large impact on their pulsation behavior because the envelope helium abundance would be greatly enhanced, impacting both the structure and the pulsational driving. More theoretical pulsation simulations are currently being performed (Templeton 1999) to help answer these questions.

5. Conclusions

We have detected 90 new δ Scuti stars in the direction of the Galactic bulge using MACHO Project photometry. The majority of these objects appear to be monoperiodic pulsators while at least ten and as many as eighteen are doubly- or multiply-periodic objects. The confirmed doubly-periodic objects appear to be fundamental-first overtone pulsators, though two of these objects have anomalous frequency ratios suggesting high metal abundances. All of the 90 objects are HADS, and the majority of these stars appear to be located in the bulge itself. Their overall behavior is very similar to field HADS and to the delta Scuti stars found by the OGLE Project, but they appear to occupy an intermediate amplitude range, between the bulk of the field LADS and the peak of the field HADS. Based on observed periods and the frequency ratios of double-mode objects, these stars are most likely pulsating in fundamental or low-overtone radial modes, with the exception of MACHO 109.20634.24 which is probably a foreground star pulsating in at least one nonradial mode. No firm conclusions can be drawn about the origin of the bulge δ Scuti stars, though their presence in a moderately old stellar population and location blueward of the main-sequence turnoff suggests a non-standard evolutionary origin. Detailed numerical studies of HADS pulsation behavior that may help us to understand their origins are now underway.

MRT thanks Siobahn Morgan for reprints of her OGLE analysis, and also thanks Joyce Guzik, Paul Bradley, and Arthur Cox of Los Alamos National Laboratory for many helpful discussions on δ Scuti star phenomenology. MRT thanks Los Alamos National Laboratory, New Mexico State University, and the New Mexico Space Grant Consortium for continued support, and is also supported under NASA Astrophysics Theory Program S-30934-F. We are very grateful for the skilled support of the technical staff at Mount Stromlo Observatory. Work at LLNL is supported by DOE contract W7405-ENG-48. Work at the CfPA is supported by NSF AST-8809616 and AST-9120005. Work at MSSSO is supported by the Australian Department of Industry, Technology and Regional Development. WJS is supported by a PPARC Advanced Fellowship. KG thanks support from DOE OJI, Sloan, and Cottrell awards. DM is supported by FONDECYT 01990440.

REFERENCES

Akerlof, C. et al. 1994. ApJ 436, 787

Alcock, C. et al. 1999. PASP, submitted.

Alcock, C. et al. 1997. ApJ 479, 119

Antonello, E. et al. 1986. A&A 169, 122

Becker, S.A. 1998. In *A Half-Century of Stellar Pulsation Interpretations*, ASP Conference Series 135, eds. P.A. Bradley and J.A. Guzik, 12

Bono, G. et al. 1997. ApJ 477, 364

Breger, M. 1998. In *A Half-Century of Stellar Pulsation Interpretations*, ASP Conference Series 135, eds. P.A. Bradley and J.A. Guzik, 460

Breger, M. 1979. PASP, 91, 5

Breger, M., & Pamyatnykh, A.A. 1998, A&A 332, 958

Cook, K.H. et al. 1995. In *Astrophysical Applications of Stellar Pulsation*, ASP Conference Series 83, eds. R.S. Stobie and P.A. Whitelock, 221

De Mey, K., Daems, K., & Sterken, C. 1998. A&A 336, 527

Gilliland, R.L. et al. 1998. ApJ 507, 818

Guzik, J.A. 1992. *Delta Scuti Star Newsletter*, 5, 8

Holtzman, J.A. et al. 1998. AJ 115, 1946

Holtzman, J.A. et al. 1993. AJ 106, 1826

McNamara, D.H. 1997. PASP 109, 1221

Minniti, D. et al. 1998. In *Proceedings of IAU Symposium 189 on Fundamental Stellar Properties: The Interaction Between Observation and Theory*, eds. T.R. Bedding, A.J. Booth, and J. Davis (Kluwer, Dordrecht), 293

Morgan, S.M., Simet, M., & Bargenquast, S. 1998. *Acta Astronomica* 48, 509

Mullan, D.J., Herr, R.B., & Bhattacharyya, S. 1992. ApJ 391, 265

Ng, Y.K. et al. 1996. A&A 310, 771

Petersen, J.O. & Christensen-Dalsgaard, J. 1996. A&A 312, 463

Petersen, J.O., & Høg, E. 1998. A&A 331, 989

Rasio, F.A. 1996. In *The Origins, Evolutions, and Destinies of Binary Stars in Clusters*, ASP Conference Series 90, eds E.F. Milone and J.-C. Mermilliod, 368

Reimann, J.D. 1994. PhD thesis, University of California, Berkeley.

Rodriguez, E. et al. 1996. A&A 307, 539

Rodriguez, E. et al. 1994. A&AS 106, 21

Sills, A.P., Bailyn, C.D., & Demarque, P. 1995. ApJ 455, L163

Simon, N.R., & Lee, A.S. 1981. ApJ 248, 291

Solano, E., & Fernley, J. 1997. A&AS 122, 131

Sterken, C., & Jaschek, C. 1996. Light Curves of Variable Stars (Cambridge University Press, Cambridge), 183

Templeton, M.R. PhD thesis, New Mexico State University, in preparation, expected May 2000.

Templeton, M.R. et al. 1998. *Delta Scuti Star Newsletter* 12, 18

Templeton, M.R. et al. 1997. AJ 114, 1592

Templeton, M.R., Bradley, P.A., & Guzik, J.A. 1999. ApJ accepted.

Templeton, M.R., Guzik, J.A., & McNamara, B.J. 1998. BAAS 193, 64.05

Udalski, A. et al. 1997. *Acta Astronomica* 47, 1

Unno, W. et al. 1989. Nonradial oscillations of stars (University of Tokyo Press, Tokyo), 2nd ed.

This manuscript was prepared with the AAS LaTeX macros v4.0.

Figure Captions

Fig. 1.— Fourier transform and phased data for 119.19574.1169 (star 1169). (a) Raw data DFT, with peaks at 9.36 and 12.09 cycles d^{-1}. (b) Raw data folded with 9.36 cycle d^{-1} frequency, showing scatter much higher than the mean error per point. (c) Data prewhitened with 9.36 cycle d^{-1} frequency, clearly showing mode at 12.09 cycles d^{-1}.

Fig. 2.— Amplitude distributions of Rodriguez et al. (1994) (top panel) and MACHO (bottom panel) δ Scuti star catalogs. The MACHO δ Scuti stars have amplitudes between the bulk of the field LADS and HADS, but are otherwise very similar to field HADS.

Fig. 3.— V amplitude versus apparent V magnitude for the 90 MACHO δ Scuti stars. Without reddening information, it is difficult to determine extinction values for these objects, but the bulk of the high amplitude stars are clustered around $V \sim 17.5$, consistent with bulge membership. The lack of bright high-amplitude objects argues for high-amplitude objects *only* in the bulge, and lower amplitude objects being a mix of bulge and foreground disk stars.

Fig. 4.— A dereddened color magnitude diagram of MACHO stars in Baade's Window (small dots) overlaid with the MACHO delta Scuti candidates (filled squares) where the dereddened W_V is defined as $V - 3.97(V - R)$. Most delta Scuti stars lie blueward majority of sources, and also lie on or blueward of the main sequence band of more recent origin. This suggests that these objects may either be a member of a more recent epoch of star formation in the bulge, or that they may be blue stragglers.

Fig. 5.— Amplitude ratios A_{N1} and phase differences ϕ_{N1} for the MACHO δ Scuti stars in V-band (a) and R-band (b). The large scatter in A_{21} as a function of period argues against this parameter being an indicator of overtone. The near-constancy of phase differences indicates that the envelope structure and pulsation behavior of these objects are similar.

Fig. 6.— Amplitude ratio $A_{21}(V)$ versus $\log \Pi_0$ for the 76 MACHO δ Scuti stars with measurable first Fourier harmonic amplitude $A_2(V)$. There appears to be no trend of light curve shape with period, which may argue against the idea that light curve shape may serve as an indicator of whether a given pulsation mode is fundamental or overtone.

Fig. 7.— Amplitude ratio $A_{21}(V)$ versus V amplitude for the 76 MACHO δ Scuti stars with measurable $A_2(V)$. There is large scatter in this relation, but the lack of low A_{21} values at higher light amplitudes

indicates that lightcurves cannot remain purely sinusoidal at higher light amplitudes.

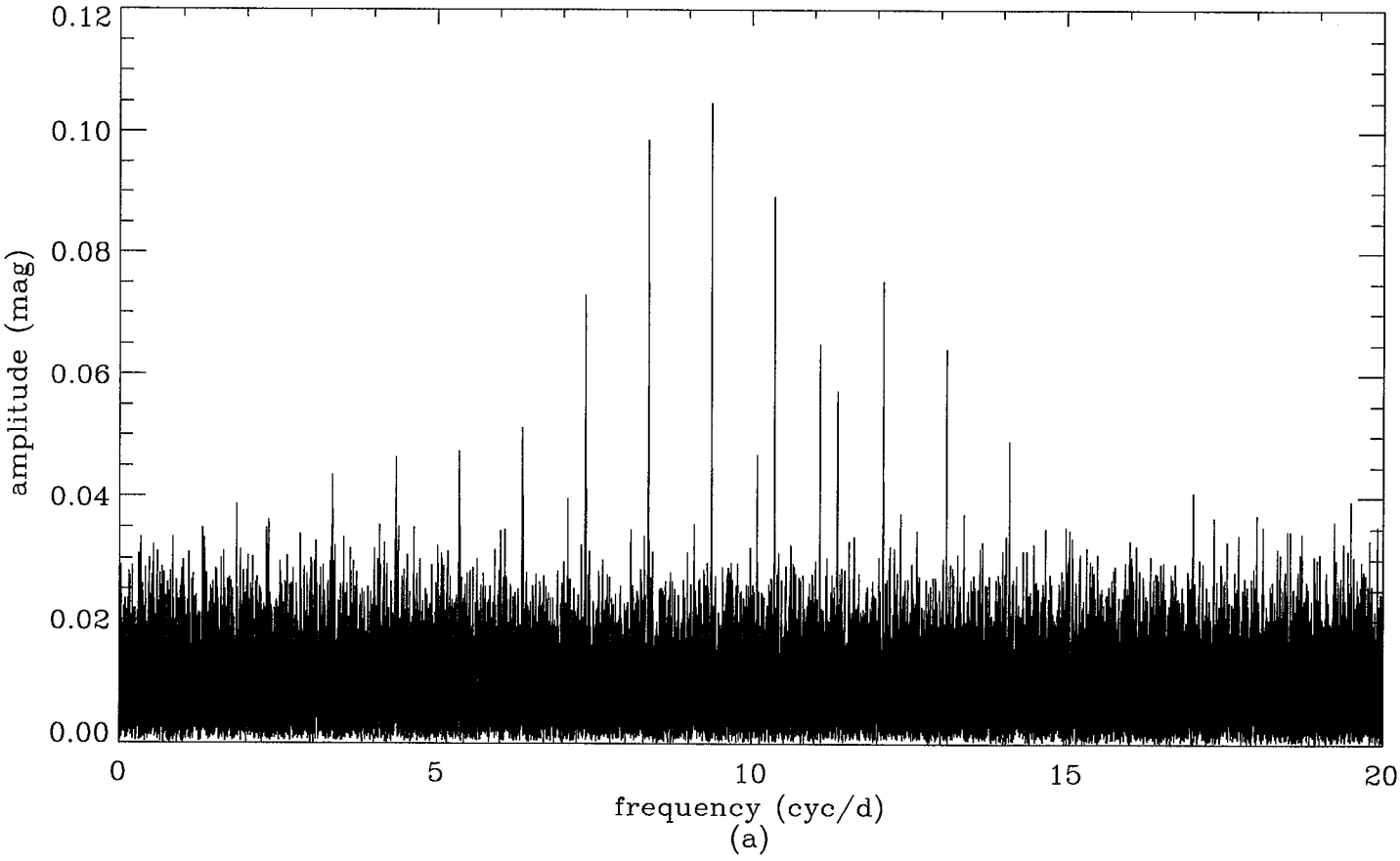
0.12
0.10
0.08
0.06
0.04
0.02
0.00
amplitude (mag)
0
5
10
15
20
frequency (cyc/d)

(a)

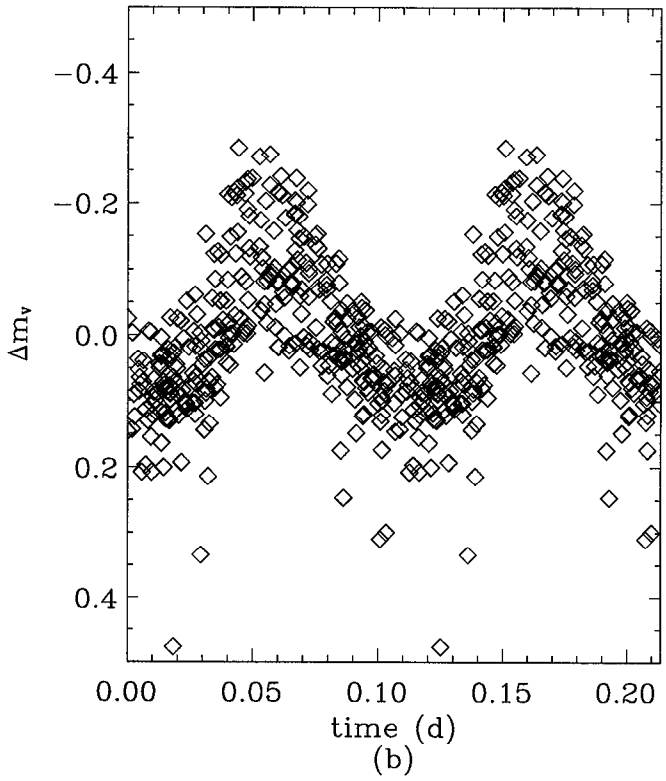
−0.4
−0.2
0.0
0.2
0.4
Δm_v
0.00
0.05
0.10
0.15
0.20
time (d)

(b)

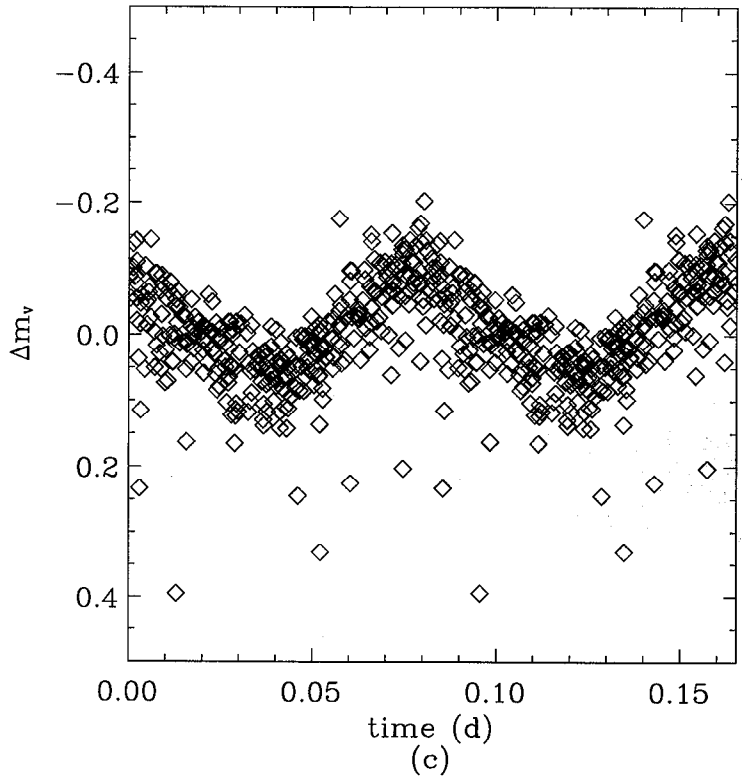
−0.4
−0.2
0.0
0.2
0.4
Δm_v
0.00
0.05
0.10
0.15
time (d)

(c)

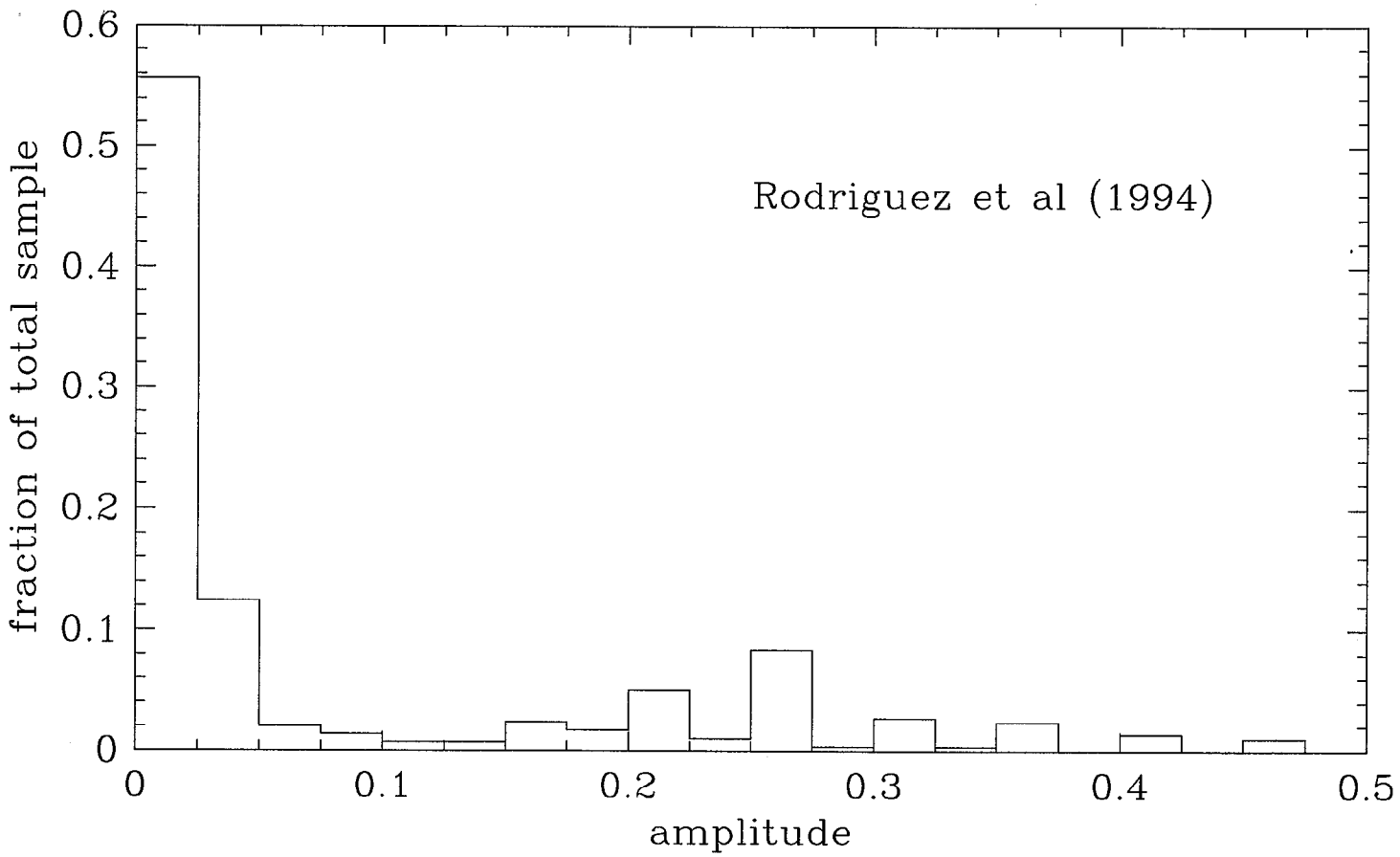
Rodriguez et al (1994)
fraction of total sample
amplitude
0.6
0.5
0.4
0.3
0.2
0.1
0
0
0.1
0.2
0.3
0.4
0.5

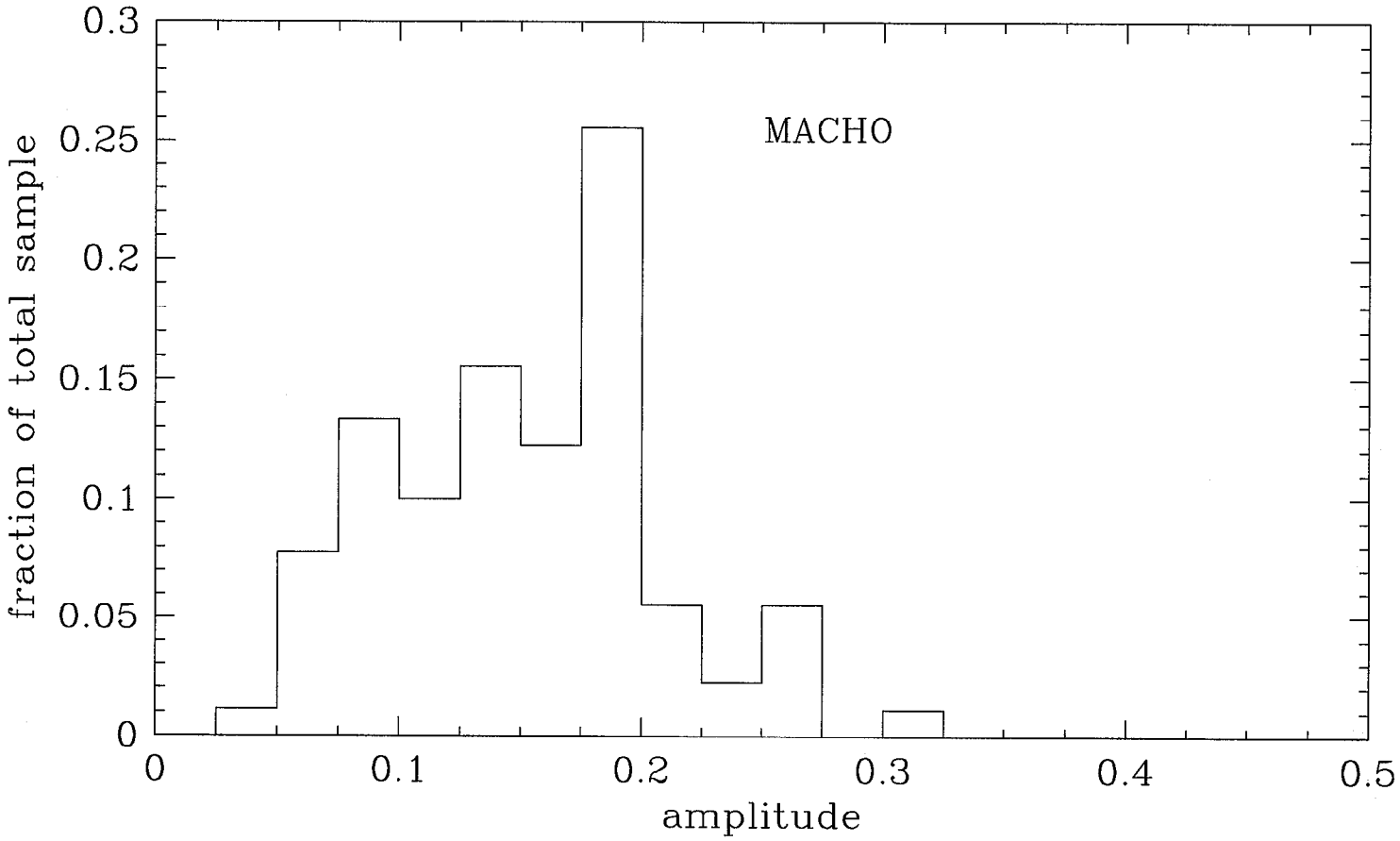
MACHO
fraction of total sample
amplitude
0.3
0.25
0.2
0.15
0.1
0.05
0
0
0.1
0.2
0.3
0.4
0.5

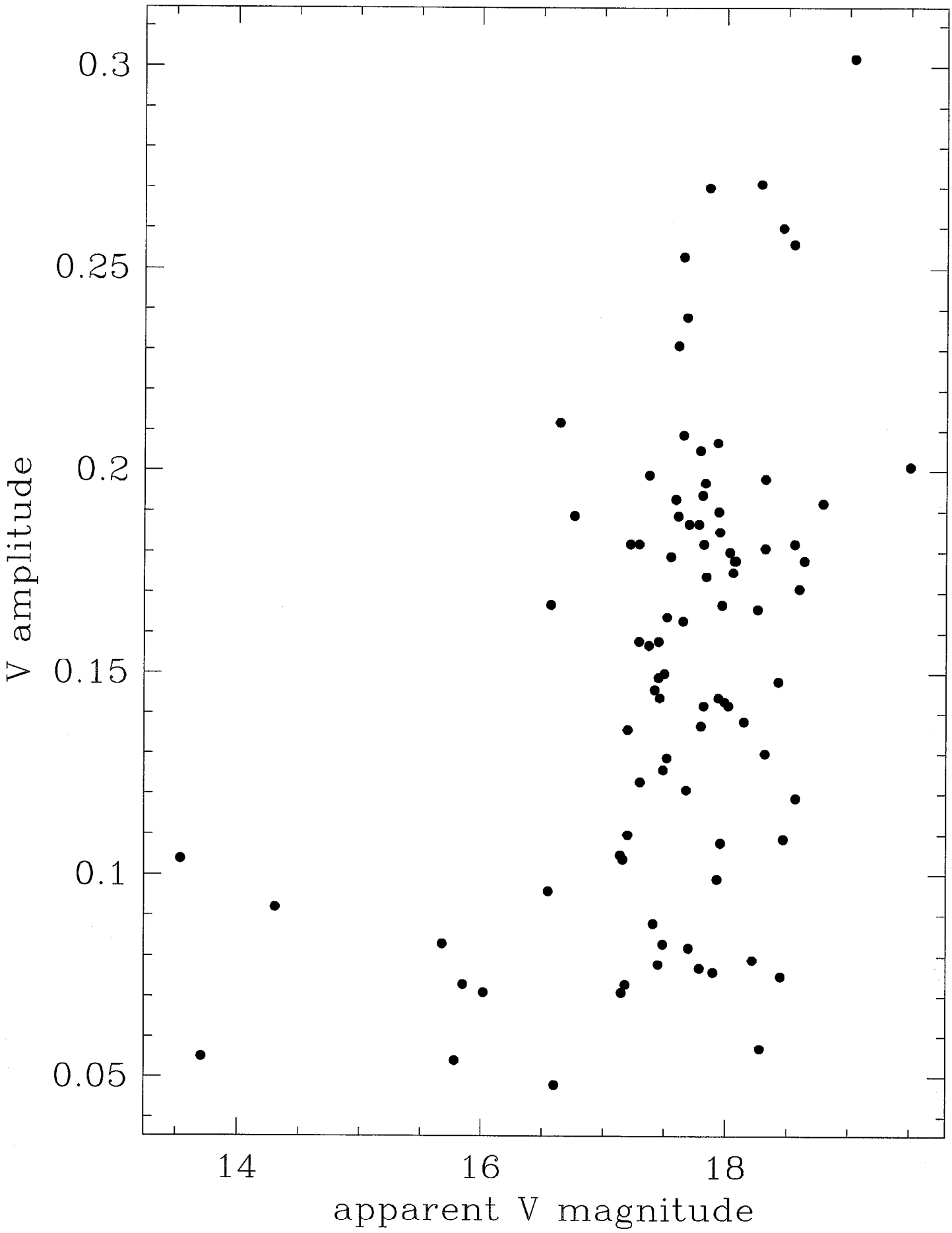
0.3
0.25
0.2
0.15
0.1
0.05
V amplitude
14
16
18
apparent V magnitude

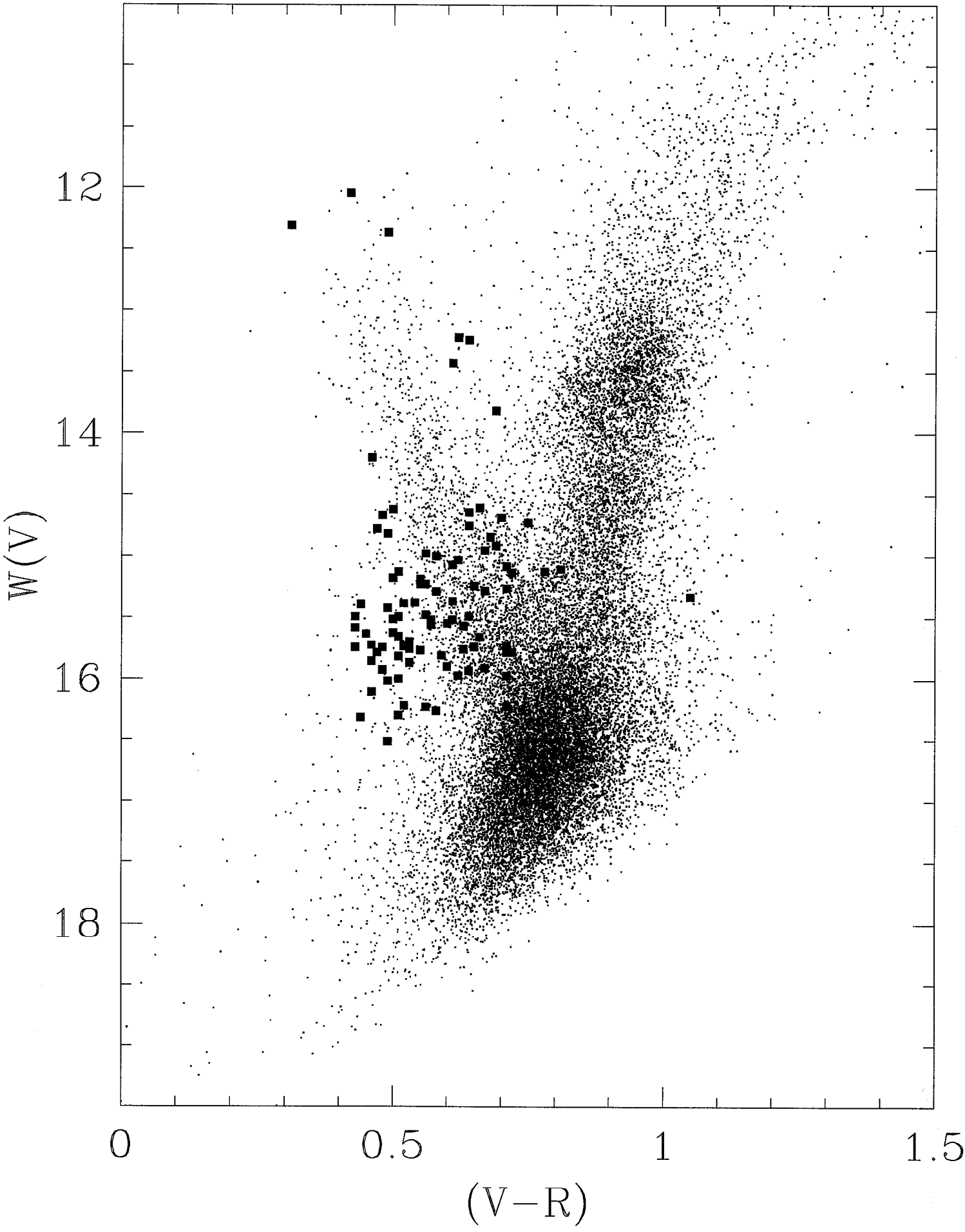
12
14
16
18
W(V)
0
0.5
1
1.5
(V−R)

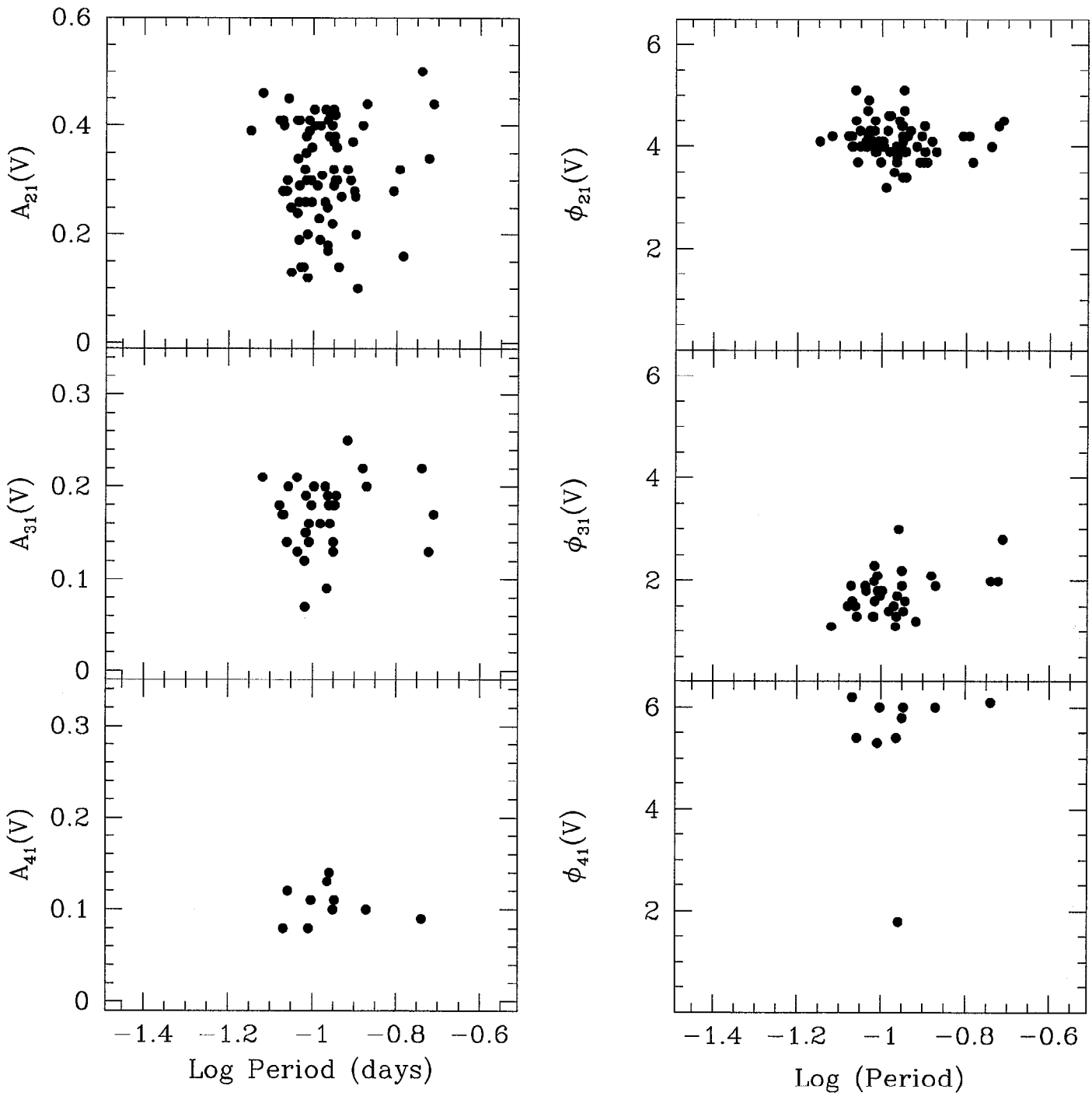
0.6
0.4
0.2
0
A_{21}(V)
0.3
0.2
0.1
0
A_{31}(V)
0.3
0.2
0.1
0
A_{41}(V)
−1.4
−1.2
−1
−0.8
−0.6
Log Period (days)
6
4
2
ϕ_{21}(V)
6
4
2
ϕ_{31}(V)
6
4
2
ϕ_{41}(V)
−1.4
−1.2
−1
−0.8
−0.6
Log (Period)

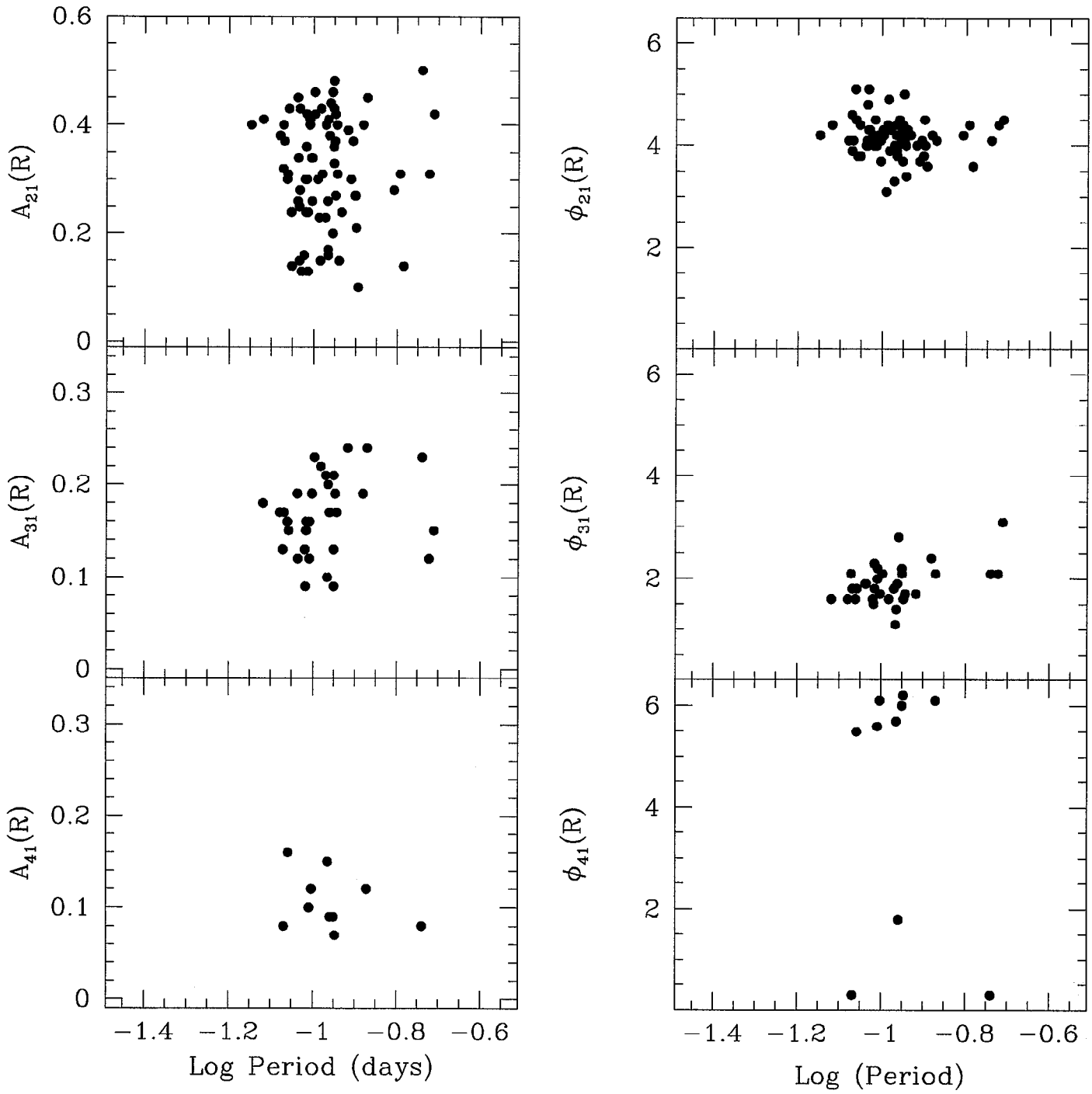
$A_{21}(R)$
$A_{31}(R)$
$A_{41}(R)$
$\phi_{21}(R)$
$\phi_{31}(R)$
$\phi_{41}(R)$
Log Period (days)
Log (Period)

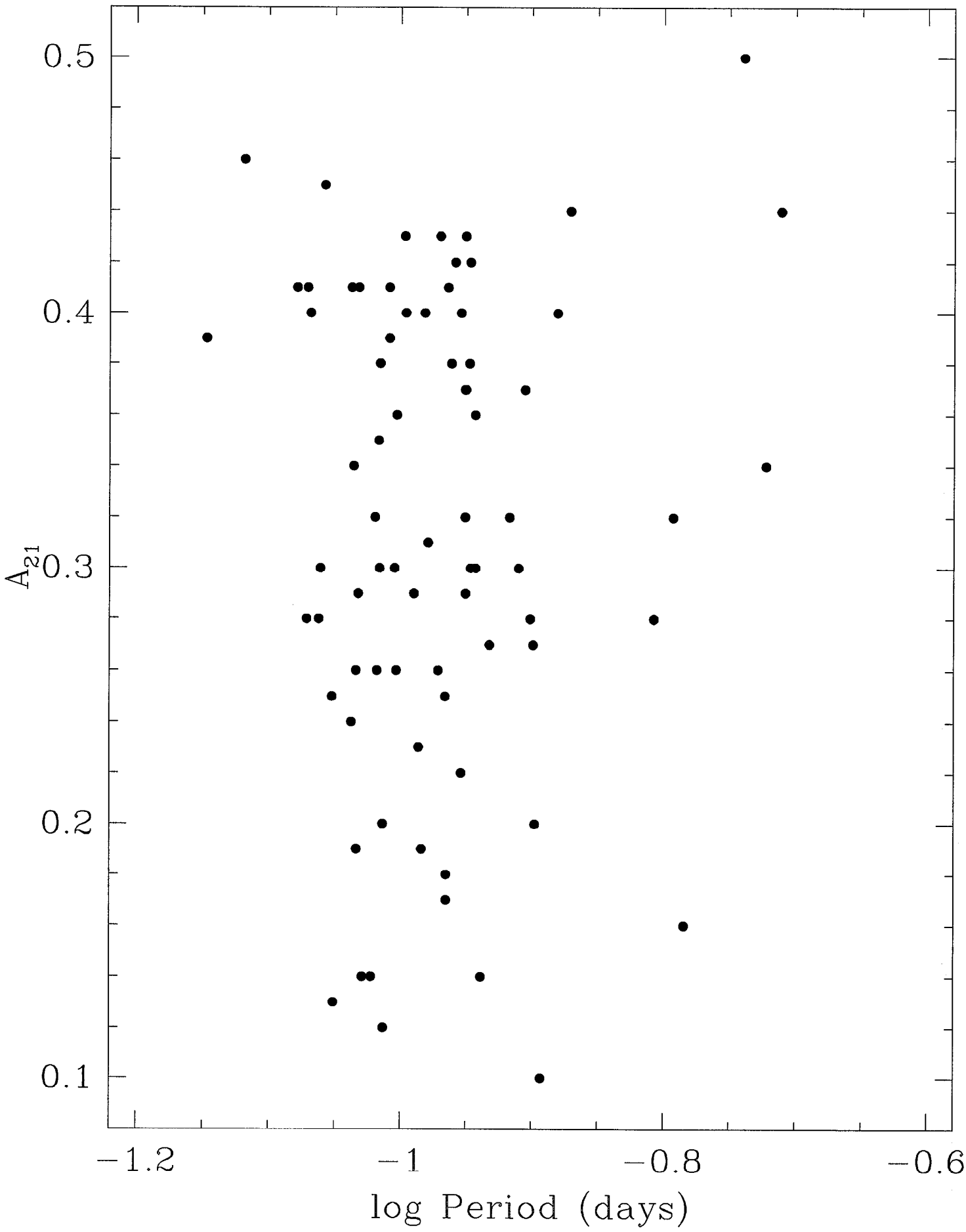
0.5
0.4
0.3
0.2
0.1
A_{21}
−1.2
−1
−0.8
−0.6
log Period (days)

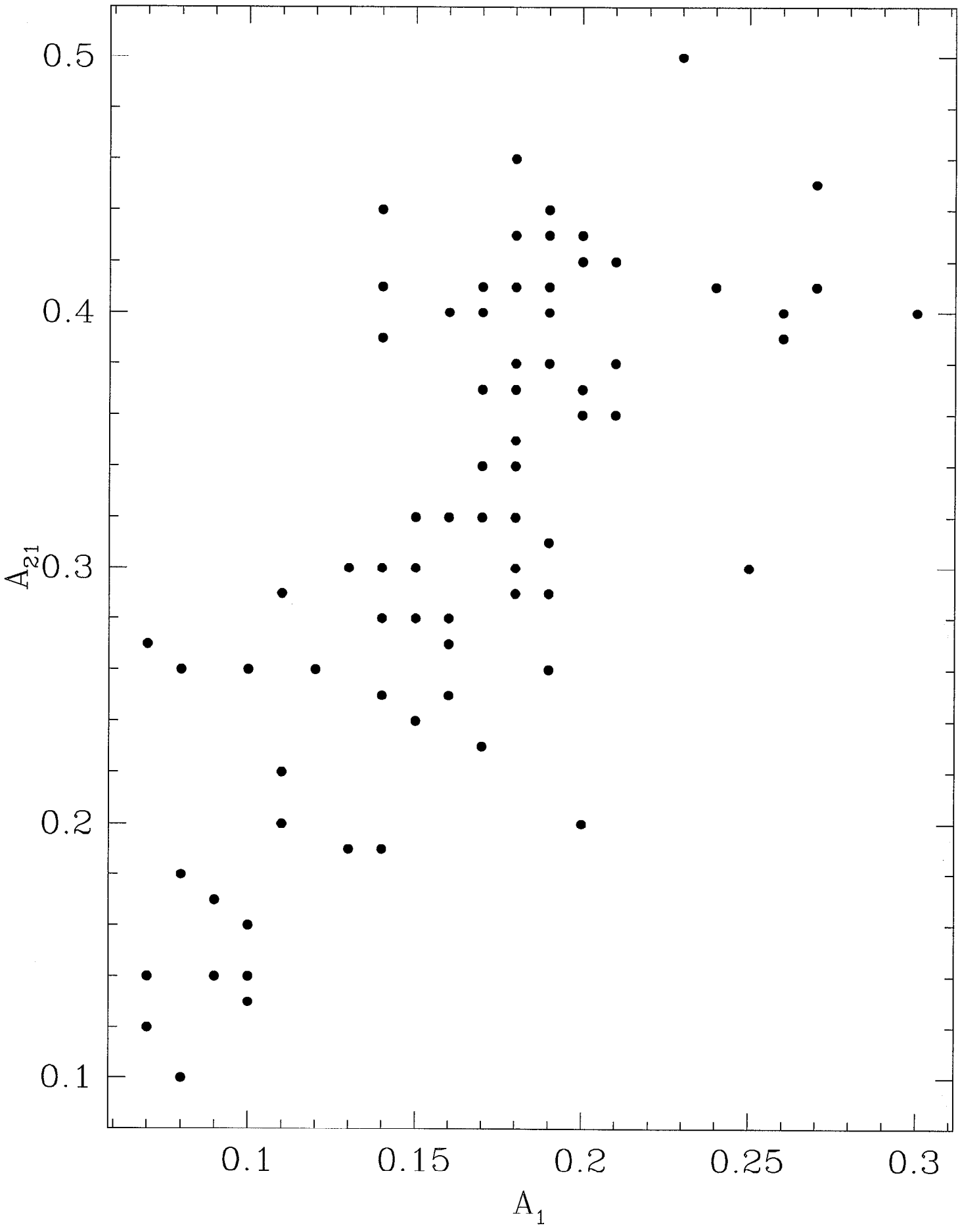
0.5
0.4
0.3
0.2
0.1
A_{21}
0.1
0.15
0.2
0.25
0.3
A_1

TABLE 1

OBSERVATIONAL DATA FOR THE 93 δ SCUTI STARS DETECTED IN THE MACHO CATALOG. N IS THE NUMBER OF POINTS IN THE DATA SET. t_0 IS THE TIME IN DAYS RELATIVE TO HJD 2449000 OF THE FIRST DATA POINT, AND t_N IS THE TOTAL LENGTH OF THE DATA SET IN DAYS. V AND R ARE THE MEAN MAGNITUDES OF THE STAR, AND $\sigma_V = \sigma_R$ IS THE MEAN PHOTOMETRIC ERROR PER POINT IN MAGNITUDES.

MACHO star	RA	declination	N	t_0 (HJD-2449000)	t_N	V	R	$\sigma_V = \sigma_R$
101.20648.1571	18:04:32.514	-27:32:43.56	405	61.2599	2197.0	18.470	17.830	0.080
101.20914.1063	18:04:56.662	-27:09:51.65	599	65.2546	2190.0	17.900	17.190	0.070
101.21305.255	18:06:03.677	-27:06:00.51	451	76.2496	1813.0	17.220	16.560	0.033
101.21436.366	18:06:12.428	-27:00:11.92	531	67.2221	1822.0	16.550	15.860	0.025
101.21437.1516	18:06:20.913	-26:57:16.42	502	66.2539	1823.0	18.550	17.840	0.103
101.21821.2017	18:07:14.770	-27:23:30.84	374	77.2988	2178.0	18.460	17.970	0.101
102.22591.871	18:09:04.476	-28:02:30.91	275	65.2818	2186.0	17.820	17.250	0.053
102.22721.762	18:09:10.172	-28:03:06.93	304	65.2818	2186.0	17.800	17.270	0.051
102.23504.1024	18:10:59.721	-27:50:50.50	221	76.2727	2175.0	17.780	17.210	0.051
103.24024.815	18:12:17.052	-27:48:44.00	126	98.2749	2133.0	17.940	17.330	0.039
103.24034.3894	18:12:15.263	-27:09:53.69	261	67.2846	2164.0	16.020	15.560	0.017
103.24284.695	18:13:01.070	-27:51:02.07	155	67.2846	2164.0	17.450	17.020	0.030
104.19990.4660	18:03:00.158	-28:06:58.18	607	54.2919	2206.0	17.700	17.140	0.044
104.20130.854	18:03:11.343	-27:26:33.60	675	54.2919	2206.0	19.500	18.450	0.198
104.20389.1202	18:03:54.048	-27:29:49.60	443	66.2445	2192.0	18.280	17.620	0.056
104.20516.955	18:04:06.584	-27:40:10.71	304	95.1988	2163.0	17.700	16.950	0.049
105.21420.2342	18:06:17.862	-28:04:54.51	538	67.2352	2191.0	18.570	17.900	0.081
105.21808.288	18:07:06.540	-28:15:15.81	275	65.2621	2186.0	17.370	16.820	0.036
105.21947.1957	18:07:32.983	-27:39:15.26	116	135.1167	1739.0	18.260	17.630	0.052
109.19721.2119	18:02:12.094	-28:41:06.34	553	79.2488	2175.0	18.640	17.920	0.087
109.19849.222	18:02:36.887	-28:48:16.74	563	76.2301	2182.0	17.540	16.860	0.039
109.19990.879	18:03:00.155	-28:06:57.84	497	46.2819	2209.0	17.800	17.280	0.044
109.20372.410	18:03:45.603	-28:37:02.06	589	46.2818	2209.0	17.290	16.650	0.035
109.20377.3241	18:03:46.890	-28:16:41.56	556	46.2818	2209.0	18.430	17.810	0.076
109.20378.2701	18:03:44.034	-28:15:06.07	557	46.2818	2209.0	16.600	16.100	0.021
109.20508.1186	18:04:10.472	-28:13:01.75	498	46.2818	1687.0	17.940	17.270	0.045
109.20634.24	18:04:33.150	-28:28:09.71	306	79.2488	2176.0	13.710	13.290	0.015
109.20638.40	18:04:18.571	-28:14:33.47	473	46.2818	1681.0	14.310	13.820	0.016
109.20762.936	18:04:46.279	-28:39:16.87	343	46.2818	2207.0	17.490	16.870	0.041
109.20764.893	18:04:42.595	-28:27:49.89	568	46.2818	2212.0	17.490	16.880	0.038
109.20890.1400	18:05:05.385	-28:45:09.15	558	46.2818	2212.0	17.860	17.330	0.073
110.22836.520	18:09:35.179	-29:02:37.48	503	65.2770	2193.0	17.820	17.170	0.047
110.22845.739	18:09:29.200	-28:27:41.07	475	65.2770	2190.0	18.220	17.440	0.057
110.23356.737	18:10:45.153	-29:03:18.19	416	65.2770	2193.0	17.680	17.220	0.057
111.23882.712	18:11:58.870	-28:37:51.25	211	67.2998	1987.0	17.610	17.110	0.036
113.18159.547	17:58:49.048	-28:49:09.21	379	44.2772	2211.0	17.460	16.760	0.038
113.19324.1134	18:01:27.936	-29:10:47.26	776	45.2741	2213.0	18.030	17.390	0.083
113.19452.883	18:01:51.464	-29:17:09.46	643	43.2815	2212.0	18.320	17.510	0.069
114.19716.1463	18:02:27.363	-29:03:07.42	516	54.2869	2206.0	18.070	17.440	0.078
114.19840.890	18:02:31.853	-29:27:03.85	634	54.2869	2206.0	17.990	17.270	0.050
114.19849.2274	18:02:36.969	-28:48:18.95	555	54.2869	2206.0	17.610	16.940	0.044
114.19969.980	18:02:52.204	-29:30:24.50	616	76.2349	2184.0	18.600	17.890	0.081
114.20108.1218	18:03:05.057	-28:52:52.68	537	54.2869	2206.0	17.550	17.090	0.036
114.20230.3899	18:03:38.323	-29:24:35.08	578	76.2349	2184.0	17.520	17.010	0.043
114.20368.797	18:03:57.216	-28:52:12.48	483	54.2868	1679.0	17.180	16.540	0.032
114.20620.159	18:04:19.436	-29:26:57.63	556	65.2306	2193.0	15.680	15.060	0.017
115.22573.263	18:09:00.480	-29:14:30.88	265	65.2909	2182.0	17.950	17.400	0.064
115.23092.1144	18:10:17.081	-29:15:56.35	220	65.2909	1617.0	18.560	17.980	0.072
115.23344.1034	18:10:44.644	-29:49:00.38	188	67.2620	2164.0	18.280	17.760	0.052
115.23474.197	18:11:07.718	-29:48:33.28	261	65.2908	2182.0	16.640	16.170	0.022
116.24123.2368	18:12:46.751	-29:52:38.11	214	79.3070	2152.0	17.370	16.880	0.027
116.24124.2364	18:12:46.005	-29:50:54.28	197	79.3070	1976.0	17.650	17.170	0.035

TABLE 1—*Continued*

MACHO star	RA	declination	N	t_0 (HJD-2449000)	t_N	V	R	$\sigma_V = \sigma_R$
116.24129.1921	18:12:37.009	-29:27:46.79	81	79.3070	2152.0	13.540	13.230	0.015
116.24131.2209	18:12:33.746	-29:20:47.10	224	95.2923	2136.0	18.060	17.620	0.046
116.24384.481	18:13:16.449	-29:49:26.99	144	83.2993	2148.0	17.290	16.860	0.027
118.17885.605	17:58:11.293	-29:45:54.04	735	54.2780	2206.0	17.650	16.960	0.053
118.18270.1993	17:58:59.510	-30:07:04.55	733	54.2780	2206.0	19.040	18.330	0.135
118.18921.1569	18:00:35.742	-30:00:26.60	225	88.1206	2164.0	18.790	18.080	0.080
119.19574.1169	18:02:00.371	-29:48:43.20	530	65.2420	2193.0	17.930	17.470	0.050
119.19835.439	18:02:36.816	-29:47:16.73	683	50.2710	2210.0	16.570	16.090	0.023
119.20351.905	18:03:42.578	-30:01:34.27	709	46.2774	2214.0	17.520	16.980	0.036
119.20738.147	18:04:52.662	-30:13:12.52	745	46.2773	2214.0	15.850	15.240	0.019
119.20738.827	18:04:41.756	-30:15:02.54	750	46.2774	2214.0	18.080	17.370	0.096
119.20742.2231	18:04:39.012	-29:58:38.74	620	46.2774	2214.0	17.840	17.330	0.057
120.21131.780	18:05:35.847	-30:02:03.15	350	70.2732	2188.0	18.150	17.560	0.047
120.21396.683	18:06:23.544	-29:41:21.44	322	70.2732	2181.0	17.420	16.970	0.034
120.21785.976	18:07:19.302	-29:46:56.22	491	65.2715	2190.0	17.450	16.890	0.042
121.21388.153	18:06:24.031	-30:13:59.51	254	65.2864	2166.0	17.680	17.170	0.038
121.21904.664	18:07:33.959	-30:31:05.90	277	65.2864	2166.0	17.970	17.440	0.043
121.22291.582	18:08:30.835	-30:42:49.11	255	76.2776	2155.0	17.790	17.270	0.034
121.22427.551	18:08:47.966	-30:19:38.73	218	65.2863	1624.0	17.590	17.010	0.036
124.21891.372	18:07:34.019	-31:21:10.71	250	65.2954	2166.0	17.160	16.660	0.024
124.21893.553	18:07:33.976	-31:13:27.74	258	65.2954	2166.0	17.650	17.180	0.030
124.21894.405	18:07:28.406	-31:08:03.54	234	65.2954	2166.0	17.140	16.700	0.023
124.22412.549	18:08:34.492	-31:15:56.53	257	65.2954	2166.0	17.500	17.000	0.036
125.23584.66	18:11:32.945	-31:08:04.43	230	83.3127	2148.0	15.780	15.140	0.019
125.23847.221	18:12:01.544	-30:57:40.03	171	83.3127	1970.0	16.760	16.270	0.035
128.21153.1181	18:05:42.128	-28:32:46.01	471	65.2670	2190.0	17.930	17.330	0.042
128.21405.697	18:06:17.374	-29:06:12.80	537	65.2670	2190.0	17.200	16.640	0.031
128.21542.753	18:06:35.933	-28:39:31.26	478	65.2670	2188.0	17.790	17.180	0.039
128.21665.609	18:06:50.829	-29:07:40.90	518	65.2670	2190.0	17.410	16.860	0.035
159.25613.963	18:16:02.854	-25:52:41.45	378	95.3081	2152.0	18.320	17.810	0.071
159.25745.544	18:16:10.473	-25:43:56.05	351	95.3081	2152.0	17.450	16.930	0.032
161.25086.954	18:14:43.392	-26:23:24.23	370	67.2799	2164.0	18.320	17.670	0.055
161.25215.1203	18:15:09.843	-26:26:50.20	389	67.2799	2164.0	18.450	17.890	0.061
162.25086.6466	18:14:43.378	-26:23:24.35	301	83.3093	2148.0	18.280	17.680	0.051
162.25343.874	18:15:16.333	-26:35:40.16	347	83.3093	2148.0	17.960	17.470	0.036
162.25348.3066	18:15:30.205	-26:14:49.49	297	83.3093	1980.0	17.810	17.280	0.035
162.25475.771	18:15:35.005	-26:26:05.45	285	96.2453	2135.0	18.020	17.510	0.050
162.25478.743	18:15:42.416	-26:13:33.21	332	83.3093	2148.0	17.830	17.350	0.053
162.25996.475	18:16:50.718	-26:23:04.82	322	95.3000	2136.0	17.200	16.770	0.026
167.24173.558	18:12:32.538	-26:35:36.88	253	67.2709	2164.0	17.300	16.720	0.038
167.24295.493	18:12:57.292	-27:07:32.64	259	66.2940	2181.0	17.150	16.640	0.025

TABLE 2

PULSATION SPECTRA FOR THE 93 δ SCUTI STARS DETECTED IN THE MACHO CATALOG. A_V AND A_R ARE THE PULSATION AMPLITUDES IN MAGNITUDES IN THE TWO PASSBANDS. P_V AND P_R ARE THE NORMALIZED POWER IN THE TWO PASSBANDS. ϕ_V AND ϕ_R ARE THE PHASES IN RADIANS RELATIVE TO t_0 GIVEN IN TABLE 1.

MACHO star	frequency (cyc d^{-1})	A_V	P_V	ϕ_V	A_R	P_R	ϕ_R
101.20648.1571	9.76699	0.109	73.66	1.73	0.091	56.40	1.74
	19.53412	0.031	9.06	0.29	0.027	6.91	0.36
101.20914.1063	6.57256	0.076	105.07	3.94	0.062	51.95	4.06
101.21305.255	8.91882	0.182	184.03	2.90	0.141	169.12	2.95
	17.83763	0.067	123.12	1.55	0.060	113.71	1.54
	26.75646	0.025	39.30	0.55	0.018	21.73	0.48
	35.67535	0.018	22.35	5.84	0.013	11.31	5.85
101.21436.366	6.08302	0.096	233.61	4.80	0.074	216.21	4.83
	12.16609	0.015	46.64	5.88	0.010	22.49	6.04
101.21437.1516	9.58501	0.256	162.99	5.42	0.202	145.24	5.44
	19.17002	0.103	78.00	0.70	0.088	67.32	0.71
	28.75506	0.042	18.70	2.29	0.045	23.66	2.13
101.21821.2017	14.02810	0.260	107.82	5.45	0.206	102.14	5.48
	28.05618	0.101	41.85	0.46	0.082	39.82	0.49
102.22591.871	8.86315	0.182	77.87	6.03	0.138	89.15	6.03
	17.72617	0.068	26.30	0.73	0.052	36.58	0.79
102.22721.762	10.10345	0.137	114.85	0.85	0.103	94.69	0.94
	20.20690	0.041	46.11	3.96	0.035	30.47	4.02
102.23504.1024	10.75762	0.187	73.57	3.83	0.137	65.97	3.87
	21.51516	0.076	39.91	2.73	0.059	32.10	2.67
103.24024.815	11.98790	0.144	51.71	5.48	0.103	46.54	5.44
	23.97577	0.059	31.71	0.44	0.039	19.57	0.51
	35.96368	0.026	13.52	2.38	0.017	5.78	2.10
103.24034.3894	10.68674	0.071	99.26	1.48	0.050	85.45	1.51
103.24284.695	10.89614	0.149	72.14	3.11	0.112	68.89	3.12
	21.79226	0.036	36.97	2.26	0.030	30.43	2.21
104.19990.4660	10.41540	0.187	252.64	1.99	0.147	236.42	1.97
	20.83081	0.048	110.03	5.99	0.036	69.67	6.12
	31.24626	0.014	14.21	4.71	0.013	12.29	4.43
104.20130.854	8.03742	0.201	111.87	4.73	0.144	162.68	4.80
	16.07489	0.074	22.52	5.24	0.053	41.54	5.50
104.20389.1202	6.34464	0.057	40.08	2.00	0.044	56.60	1.89
	8.45177	0.038	21.97	3.89	0.026	27.51	3.89
104.20516.955	9.39176	0.082	38.16	1.95	0.050	56.52	1.97
105.21420.2342	10.53760	0.119	114.27	1.66	0.090	114.35	1.67

TABLE 2—*Continued*

MACHO star	frequency (cyc d^{-1})	A_V	P_V	ϕ_V	A_R	P_R	ϕ_R
105.21808.288	8.77358	0.199	108.40	0.18	0.155	105.60	0.22
	17.54723	0.072	67.21	2.73	0.061	72.23	2.77
	26.32082	0.038	35.66	5.22	0.026	25.05	5.24
105.21947.1957	8.92978	0.166	51.01	4.99	0.132	50.01	5.14
	17.85964	0.062	23.31	0.32	0.048	21.26	0.33
109.19721.2119	8.25999	0.178	150.51	1.72	0.128	154.21	1.80
	16.51999	0.057	33.73	5.75	0.050	52.60	5.84
	24.78003	0.045	24.17	3.98	0.031	25.14	3.73
109.19849.222	5.48653	0.224	203.24	4.03	0.178	190.59	4.08
	10.97309	0.107	179.21	3.93	0.084	139.00	3.92
	16.45964	0.057	137.31	3.60	0.044	74.11	3.56
	21.94625	0.022	39.84	4.21	0.017	14.28	3.96
	27.43266	0.014	18.54	3.36	0.008	3.33	3.30
	32.91926	0.016	24.70	4.06	0.013	9.14	4.34
109.19990.879	10.41540	0.184	206.28	4.58	0.148	180.28	4.60
	20.83082	0.045	94.85	5.14	0.039	51.05	5.14
109.20372.410	7.91879	0.158	245.45	1.29	0.125	238.40	1.32
	15.83754	0.042	107.05	4.45	0.033	90.50	4.47
109.20377.3241	8.93057	0.148	185.05	2.81	0.113	153.35	2.87
	17.86111	0.048	57.62	1.47	0.041	44.71	1.42
109.20378.2701	9.63835	0.048	146.23	3.65	0.038	109.47	3.75
	9.65558	0.030	122.26	3.43	0.023	65.55	3.43
	10.13476	0.011	30.77	2.77	0.009	12.28	2.53
109.20508.1186	7.42386	0.190	180.52	4.26	0.144	168.28	4.34
	14.84776	0.084	122.54	4.67	0.065	101.07	4.63
	22.27159	0.039	51.49	4.63	0.035	48.87	4.59
	29.69555	0.018	14.45	4.82	0.018	15.72	4.98
109.20634.24	5.61171	0.055	106.73	1.89	0.043	87.52	1.87
	5.47079	0.019	35.78	2.81	0.014	21.60	2.86
	6.92653	0.015	31.11	5.51	0.012	18.21	5.41
	6.85830	0.013	29.24	4.55	0.012	18.39	4.63
109.20638.40	8.68086	0.092	200.90	5.01	0.073	194.28	5.03
	17.36172	0.013	29.45	5.84	0.011	27.36	5.76
	11.55858	0.013	33.92	3.77	0.013	45.37	3.79
109.20762.936	8.76478	0.126	139.10	2.02	0.093	104.96	2.00
	17.52964	0.038	55.86	0.62	0.029	23.77	0.62
109.20764.893	5.24848	0.083	201.39	5.11	0.071	190.38	5.12
109.20890.1400	10.19946	0.270	216.40	4.11	0.223	197.98	4.14
	20.39890	0.112	166.33	4.06	0.089	108.34	4.05

TABLE 2—*Continued*

MACHO star	frequency (cyc d^{-1})	A_V	P_V	ϕ_V	A_R	P_R	ϕ_R
	30.59832	0.044	59.35	3.98	0.037	29.01	4.14
	40.79787	0.021	16.63	4.82	0.022	11.93	4.70
110.22836.520	10.19437	0.142	166.97	1.71	0.108	139.72	1.78
	20.38871	0.055	81.16	5.69	0.044	56.48	5.68
	30.58303	0.020	16.49	3.35	0.013	6.31	3.17
110.22845.739	9.71773	0.079	77.83	2.21	0.060	92.63	2.20
110.23356.737	9.20061	0.238	146.60	0.79	0.194	137.05	0.81
	18.40125	0.099	95.47	4.08	0.079	72.40	4.12
	27.60189	0.046	43.48	1.12	0.039	29.15	1.05
	36.80247	0.032	25.92	4.08	0.029	19.45	3.87
	46.00316	0.020	11.43	0.95	0.014	4.32	0.78
111.23882.712	8.92077	0.189	83.38	5.18	0.136	71.34	5.21
	17.84153	0.082	68.47	6.26	0.065	49.27	6.21
	26.76228	0.034	36.44	1.05	0.028	17.63	1.01
113.18159.547	5.14025	0.144	125.52	5.89	0.114	125.42	5.91
	10.28048	0.064	81.52	0.97	0.048	75.57	1.04
	15.42074	0.024	20.96	2.36	0.017	16.40	2.11
113.19324.1134	9.32737	0.180	208.77	2.60	0.146	186.42	2.66
	18.65477	0.078	90.49	1.35	0.059	60.77	1.36
	27.98215	0.036	25.25	0.00	0.030	19.20	6.20
113.19452.883	8.12942	0.130	163.79	1.85	0.105	158.69	1.84
	16.25885	0.039	30.14	0.00	0.031	27.30	6.26
114.19716.1463	8.92315	0.178	187.40	5.97	0.138	120.40	6.01
	17.84625	0.051	56.55	1.21	0.046	24.62	1.30
	26.76942	0.024	15.42	3.09	0.013	2.18	3.27
114.19840.890	7.96395	0.143	165.81	5.08	0.117	140.29	5.12
	10.33167	0.052	45.31	1.38	0.033	19.75	1.37
	15.92791	0.040	31.25	0.12	0.032	19.82	0.12
	18.29552	0.029	18.25	1.74	0.023	11.16	1.82
114.19849.2274	5.48654	0.231	189.90	0.15	0.171	168.38	0.17
	10.97308	0.115	166.27	2.60	0.086	116.91	2.53
	16.45964	0.051	86.51	4.75	0.040	45.27	4.69
	21.94612	0.021	21.43	0.74	0.014	6.45	0.41
	27.43273	0.015	12.53	3.64	0.011	4.75	3.75
	32.91918	0.019	18.55	6.19	0.021	15.60	0.05
	38.40565	0.015	13.39	1.24	0.012	5.45	1.06
114.19969.980	9.68320	0.171	178.17	2.24	0.133	201.18	2.23
	19.36638	0.039	21.57	0.13	0.030	29.44	0.08
	12.52957	0.037	20.87	1.21	0.029	31.00	1.24
114.20108.1218	10.85572	0.179	208.78	3.15	0.143	179.05	3.20

TABLE 2—*Continued*

MACHO star	frequency (cyc d^{-1})	A_V	P_V	ϕ_V	A_R	P_R	ϕ_R
	21.71143	0.062	125.22	2.29	0.049	68.17	2.32
	32.56717	0.024	35.54	1.40	0.018	11.98	1.41
	13.79556	0.013	11.53	5.25	0.016	10.49	5.41
114.20230.3899	9.63362	0.129	208.69	5.37	0.110	211.05	5.42
	19.26726	0.024	24.99	6.18	0.017	18.05	5.93
114.20368.797	8.55258	0.073	132.50	3.13	0.056	119.15	3.13
	10.82242	0.026	35.75	6.15	0.021	31.67	0.10
	17.10518	0.020	25.04	1.99	0.014	15.50	2.10
114.20620.159	7.81557	0.083	257.31	0.66	0.068	229.63	0.67
	15.63113	0.009	55.19	3.90	0.007	15.48	4.03
115.22573.263	10.89872	0.185	85.22	5.70	0.157	59.50	5.70
	14.11001	0.047	15.11	0.79	0.047	9.64	0.83
115.23092.1144	10.89628	0.182	75.84	4.98	0.144	70.92	5.01
	21.79259	0.075	36.78	5.89	0.065	36.52	5.98
	32.68885	0.039	14.71	0.46	0.028	10.04	0.60
115.23344.1034	11.42065	0.271	72.72	3.68	0.229	71.28	3.73
	22.84133	0.123	57.05	3.63	0.098	46.94	3.66
	34.26200	0.055	26.80	3.44	0.035	11.34	3.11
	45.68265	0.034	14.10	3.05	0.037	14.23	3.08
115.23474.197	10.06542	0.212	104.63	0.76	0.170	101.74	0.79
	20.13082	0.077	75.67	3.79	0.058	58.86	3.80
	30.19627	0.039	48.95	0.61	0.032	33.02	0.64
	40.26164	0.024	29.85	3.33	0.020	16.76	3.37
	50.32710	0.013	11.54	5.98	0.011	5.59	5.62
116.24123.2368	8.99396	0.157	77.06	0.67	0.115	68.00	0.69
	17.98788	0.063	52.62	3.61	0.053	44.88	3.60
116.24124.2364	10.37310	0.253	80.08	3.20	0.198	80.73	3.23
	20.74616	0.075	32.66	1.93	0.060	34.46	1.92
	31.11929	0.049	20.82	1.01	0.031	15.40	1.05
116.24129.1921	12.07559	0.104	35.44	0.97	0.077	33.95	1.03
116.24131.2209	11.76842	0.175	73.61	1.75	0.131	64.21	1.81
	23.53677	0.072	36.73	5.78	0.052	23.72	5.98
116.24384.481	11.50557	0.182	59.22	4.37	0.145	55.56	4.37
	23.01107	0.054	34.11	4.23	0.044	25.01	4.25
	14.88981	0.029	19.96	4.09	0.023	10.48	4.09
	34.51673	0.025	20.68	5.36	0.023	12.46	5.25
118.17885.605	6.41524	0.163	254.33	0.80	0.136	252.62	0.79
	12.83047	0.045	65.21	3.67	0.038	66.06	3.68

TABLE 2—*Continued*

MACHO star	frequency (cyc d^{-1})	A_V	P_V	ϕ_V	A_R	P_R	ϕ_R
118.18270.1993	7.59498	0.302	240.95	4.31	0.247	244.41	4.37
	15.18999	0.122	118.99	4.55	0.098	119.74	4.58
	22.78497	0.065	51.24	4.53	0.047	41.83	4.45
118.18921.1569	9.52864	0.192	59.67	4.10	0.166	55.90	4.11
	19.05715	0.059	11.58	3.59	0.052	10.52	3.87
119.19574.1169	9.35930	0.099	93.33	0.98	0.080	70.28	0.95
	12.08875	0.087	116.48	2.32	0.074	82.74	2.44
	18.71868	0.025	17.45	4.77	0.019	7.66	4.89
	21.44804	0.024	17.55	5.27	0.027	16.62	5.19
119.19835.439	5.27501	0.167	270.19	2.85	0.130	186.41	2.84
	10.55000	0.056	154.02	1.33	0.040	40.10	1.23
	15.82508	0.022	42.89	0.25	0.015	6.67	0.11
	8.67222	0.021	48.07	2.23	0.021	12.14	2.40
	8.61755	0.018	39.41	2.73	0.018	9.67	2.65
119.20351.905	6.20065	0.164	241.97	2.34	0.131	243.77	2.39
	12.40131	0.053	88.91	0.49	0.041	85.69	0.40
119.20738.147	10.30463	0.073	316.04	2.75	0.058	280.05	2.78
	20.60925	0.009	32.13	1.58	0.008	21.44	1.56
119.20738.827	10.38803	0.178	241.68	1.27	0.143	230.72	1.33
	20.77608	0.062	94.96	4.90	0.051	85.45	4.88
	31.16403	0.027	26.50	1.84	0.021	19.55	1.65
119.20742.2231	9.90682	0.174	177.21	6.08	0.142	160.34	6.14
	19.81363	0.070	69.80	1.83	0.060	62.41	1.77
120.21131.780	11.53958	0.138	122.84	0.93	0.102	128.61	0.97
	23.07906	0.039	33.97	3.08	0.030	44.50	3.11
120.21396.683	8.84571	0.146	96.60	4.26	0.130	122.99	4.29
	17.69134	0.044	21.08	3.80	0.036	36.05	3.55
120.21785.976	9.24373	0.158	202.91	0.50	0.121	176.87	0.55
	18.48747	0.039	66.28	3.29	0.031	41.68	3.22
	27.73122	0.014	11.96	0.42	0.012	7.53	0.59
	12.98294	0.015	14.23	1.54	0.013	9.02	1.66
121.21388.153	10.07095	0.121	94.58	2.08	0.096	88.12	2.05
	20.14191	0.032	26.26	0.50	0.025	18.84	0.37
121.21904.664	10.45362	0.167	110.76	0.44	0.131	98.79	0.50
	20.90727	0.054	58.37	3.21	0.040	31.04	3.33
	31.36095	0.020	13.90	0.01	0.017	7.13	6.16
121.22291.582	10.36103	0.193	98.47	1.19	0.153	90.66	1.22
	20.72208	0.073	77.84	4.70	0.064	64.06	4.62
	31.08312	0.030	31.94	1.93	0.023	15.64	1.82

TABLE 2—*Continued*

MACHO star	frequency (cyc d^{-1})	A_V	P_V	ϕ_V	A_R	P_R	ϕ_R
121.22427.551	10.31268	0.205	71.99	3.00	0.157	92.52	3.04
	23.48304	0.052	11.70	3.52	0.034	20.21	3.57
	13.17041	0.042	8.50	5.69	0.030	18.72	5.50
	20.62540	0.041	8.87	2.00	0.038	38.53	2.05
124.21891.372	10.52586	0.104	104.77	3.78	0.082	106.10	3.78
	21.05169	0.015	20.10	3.50	0.013	23.08	3.40
124.21893.553	9.14492	0.209	104.16	6.17	0.166	99.12	6.23
	18.28987	0.079	71.19	2.19	0.064	59.06	2.22
	27.43478	0.038	38.08	4.25	0.028	20.96	4.18
124.21894.405	11.24819	0.105	101.87	2.87	0.086	97.93	2.88
	22.49641	0.014	27.76	1.70	0.012	23.37	1.96
124.22412.549	11.78423	0.150	100.27	0.93	0.112	78.87	1.04
	23.56844	0.042	37.66	3.96	0.036	19.97	3.73
	35.35268	0.025	18.28	0.94	0.014	3.98	0.99
125.23584.66	11.60383	0.054	75.05	3.13	0.039	59.93	3.21
125.23847.221	10.76675	0.189	79.85	2.65	0.148	77.71	2.72
	21.53344	0.054	46.74	1.09	0.041	38.60	1.12
128.21153.1181	8.84936	0.207	174.84	6.27	0.166	177.36	0.06
	17.69873	0.086	126.09	2.31	0.069	138.48	2.34
	26.54812	0.037	51.13	4.86	0.032	71.64	4.87
	35.39742	0.023	25.08	0.21	0.012	15.56	0.36
128.21405.697	7.89679	0.110	217.10	5.20	0.083	206.69	5.21
	15.79357	0.022	48.41	0.19	0.018	44.29	0.12
128.21542.753	10.80603	0.077	106.22	2.53	0.064	95.96	2.58
	8.32973	0.051	83.75	2.70	0.044	74.95	2.90
	21.61200	0.020	20.83	0.31	0.016	15.30	0.37
	19.13576	0.020	21.38	1.32	0.018	20.43	1.30
128.21665.609	9.22620	0.088	181.69	5.06	0.073	128.12	5.13
	18.45240	0.015	19.71	6.19	0.012	6.71	5.89
159.25613.963	13.13692	0.181	123.93	4.77	0.142	114.04	4.84
	26.27383	0.082	68.99	5.35	0.059	45.71	5.31
	39.41077	0.038	23.45	0.61	0.026	12.01	0.33
159.25745.544	9.22971	0.078	125.22	0.80	0.063	132.68	0.80
	18.45935	0.014	13.33	4.15	0.011	14.84	3.96
161.25086.954	9.08552	0.198	114.68	2.67	0.161	132.78	2.67
	18.17099	0.083	50.10	0.87	0.071	86.20	0.86
	27.25643	0.032	10.32	5.05	0.027	22.14	5.18
	36.34185	0.027	7.63	2.57	0.014	7.22	2.62

TABLE 2—*Continued*

MACHO star	frequency (cyc d^{-1})	A_V	P_V	ϕ_V	A_R	P_R	ϕ_R
161.25215.1203	11.76963	0.075	61.60	1.01	0.066	59.30	1.05
162.25343.874	8.98622	0.108	114.48	1.15	0.086	91.82	1.15
	11.64074	0.041	59.28	0.59	0.034	34.27	0.60
	17.97240	0.024	30.80	4.21	0.017	10.61	4.20
162.25348.3066	11.70606	0.194	118.04	2.48	0.144	103.00	2.51
	23.41209	0.078	89.71	0.93	0.053	45.57	0.95
	35.11815	0.033	39.98	5.80	0.025	14.22	5.74
	46.82417	0.016	13.29	3.76	0.012	3.76	3.40
162.25475.771	11.27268	0.142	100.17	2.37	0.111	83.44	2.36
	14.48269	0.040	29.71	0.61	0.031	16.94	0.38
	22.54535	0.035	29.83	0.47	0.027	14.46	0.36
	14.40240	0.028	23.90	1.95	0.022	10.52	1.69
	25.75540	0.019	13.65	5.23	0.017	7.00	5.68
162.25478.743	9.92486	0.197	120.77	3.95	0.157	87.64	4.01
	19.84970	0.084	80.02	3.80	0.073	39.81	3.75
	29.77457	0.039	32.44	3.76	0.036	12.84	3.68
162.25086.6466	9.08551	0.206	113.35	4.94	0.154	103.10	4.94
	18.17100	0.083	71.22	5.44	0.065	57.59	5.44
	27.25651	0.037	28.11	0.08	0.035	27.02	0.04
162.25996.475	10.80128	0.136	133.14	6.23	0.114	114.46	6.23
	21.60252	0.026	27.13	2.00	0.017	9.06	2.14
	10.80047	0.029	41.27	0.65	0.028	25.81	0.70
167.24173.558	8.59703	0.123	88.16	0.42	0.082	52.00	0.38
167.24295.493	9.53194	0.071	95.70	1.75	0.058	90.39	1.75

TABLE 3A

V-BAND FOURIER AMPLITUDE RATIOS AND PHASE DIFFERENCES FOR THE 79 OBJECTS IN OUR SAMPLE OF MACHO DELTA SCUTI STARS HAVING A FIRST FOURIER HARMONIC (A_2). A_{n1} IS THE RATIO OF n-TH TO FUNDAMENTAL FOURIER HARMONIC AMPLITUDES. ϕ_{n1} IS THE NORMALIZED PHASE DIFFERENCE $\phi_n - n\phi 1$ IN RADIANS.

MACHO Star #	ν	A_1	ϕ_1	A_{21}	ϕ_{21}	A_{31}	ϕ_{31}	A_{41}	ϕ_{41}	A_{51}	ϕ_{51}	A_{61}	ϕ_{61}	A_{71}	ϕ_{71}
101.20648.1571	9.766988	0.11	1.7	0.29	3.2										
101.21305.255	8.918816	0.18	2.9	0.37	4.2	0.14	1.9	0.10	5.8						
101.21436.366	6.083023	0.10	4.8	0.16	3.7										
101.21437.1516	9.585009	0.26	5.4	0.40	3.9	0.16	1.4								
101.21821.2017	14.028103	0.26	5.4	0.39	4.1										
102.22591.871	8.863148	0.18	6.0	0.38	5.1										
102.22721.762	10.103451	0.14	0.8	0.30	4.0										
102.23504.1024	10.757620	0.19	3.8	0.41	4.9										
103.24024.815	11.987896	0.14	5.5	0.41	4.2	0.18	1.5								
103.24034.3894	10.686740	0.07	1.5	0.14	4.3										
103.24284.695	10.896136	0.15	3.1	0.24	4.0										
104.19990.4660	10.415403	0.19	2.0	0.26	4.3	0.07	1.3								
104.20130.854	8.037423	0.20	4.7	0.37	4.2										
105.21808.288	8.773583	0.20	0.2	0.36	3.9	0.19	1.6								
105.21947.1957	8.929778	0.17	5.0	0.37	3.4										
109.19721.2119	8.259985	0.18	1.7	0.32	4.0	0.25	1.2								
109.19849.222	5.486534	0.22	4.0	0.48	4.1	0.25	2.2	0.10	5.6	0.06	4.2	0.07	1.3		
109.19990.879	10.415396	0.18	4.6	0.25	4.0										
109.20372.410	7.918786	0.16	1.3	0.27	4.4										
109.20377.3241	8.930567	0.15	2.8	0.32	4.2										
109.20508.1186	7.423864	0.19	4.3	0.44	3.9	0.20	1.9	0.10	6.0						
109.20638.40	8.680859	0.09	5.0	0.14	4.2										
109.20762.936	8.764776	0.13	2.0	0.30	3.4										
109.20890.1400	10.199457	0.27	4.1	0.41	4.1	0.16	2.1	0.08	5.3						
110.22836.520	10.194366	0.14	1.7	0.39	4.0	0.14	1.8								
110.23356.737	9.200613	0.24	0.8	0.41	3.8	0.19	1.3	0.13	5.4	0.09	3.0				
111.23882.712	8.920773	0.19	5.2	0.43	4.1	0.18	1.9								
113.18159.547	5.140253	0.14	5.9	0.44	4.5	0.17	2.8								
113.19324.1134	9.327369	0.18	2.6	0.43	3.9	0.20	1.5								
113.19452.883	8.129420	0.13	1.9	0.30	3.7										
114.19716.1463	8.923152	0.18	6.0	0.29	4.4	0.13	2.2								
114.19840.890	7.963950	0.14	5.1	0.28	3.7										
114.19849.2274	5.486536	0.23	0.2	0.50	4.0	0.22	2.0	0.09	6.1	0.06	3.4	0.08	1.0	0.07	6.1
114.19969.980	9.683205	0.17	2.2	0.23	4.3										
114.20108.1218	10.855722	0.18	3.2	0.34	4.0	0.13	1.8								
114.20230.3899	9.633618	0.13	5.4	0.19	4.6										
114.20368.797	8.552585	0.07	3.1	0.27	4.3										
114.20620.159	7.815573	0.08	0.7	0.10	3.7										
115.23092.1144	10.896281	0.18	5.0	0.41	4.1	0.21	1.9								
115.23344.1034	11.420648	0.27	3.7	0.45	3.7	0.20	1.3	0.12	5.4						
115.23474.197	10.065422	0.21	0.8	0.36	4.0	0.18	1.7	0.11	6.0	0.06	4.1				
116.24123.2368	8.993959	0.16	0.7	0.40	4.0										
116.24124.2364	10.373105	0.25	3.2	0.30	4.5	0.19	2.3								
116.24131.2209	11.768418	0.17	1.8	0.41	4.0										
116.24384.481	11.505569	0.18	4.4	0.30	4.5	0.14	1.5								
118.17885.605	6.415236	0.16	0.8	0.28	4.2										
118.18270.1993	7.594984	0.30	4.3	0.40	4.1	0.22	2.1								
118.18921.1569	9.528644	0.19	4.1	0.31	4.6										
119.19574.1169	9.359298	0.10	1.0	0.26	3.5										
119.19835.439	5.275013	0.17	2.8	0.34	4.4	0.13	2.0								
119.20351.905	6.200649	0.16	2.3	0.32	4.2										
119.20738.147	10.304626	0.07	2.7	0.12	3.9										

TABLE 3A—*Continued*

MACHO Star #	ν	A_1	ϕ_1	A_{21}	ϕ_{21}	A_{31}	ϕ_{31}	A_{41}	ϕ_{41}	A_{51}	ϕ_{51}	A_{61}	ϕ_{61}	A_{71}	ϕ_{71}
119.20738.827	10.388032	0.18	1.3	0.35	3.9	0.15	2.0								
119.20742.2231	9.906815	0.17	6.1	0.40	4.0										
120.21131.780	11.539582	0.14	0.9	0.28	5.1										
120.21396.683	8.845706	0.15	4.3	0.30	4.7										
120.21785.976	9.243728	0.16	0.5	0.25	4.0	0.09	1.1								
121.21388.153	10.070951	0.12	2.1	0.26	3.7										
121.21904.664	10.453621	0.17	0.4	0.32	4.0	0.12	1.3								
121.22291.582	10.361032	0.19	1.2	0.38	4.0	0.15	1.6								
121.22427.551	10.312683	0.20	3.0	0.20	4.0										
124.21891.372	10.525859	0.10	3.8	0.14	4.1										
124.21893.553	9.144923	0.21	6.2	0.38	3.9	0.18	1.7								
124.21894.405	11.248193	0.10	2.9	0.13	4.0										
124.22412.549	11.784227	0.15	0.9	0.28	4.2	0.17	1.9								
125.23847.221	10.766746	0.19	2.6	0.29	4.2										
128.21153.1181	8.849363	0.21	6.3	0.42	3.9	0.18	1.4	0.11	6.0						
128.21405.697	7.896792	0.11	5.2	0.20	3.9										
128.21542.753	10.806030	0.08	2.5	0.26	4.7										
128.21665.609	9.226202	0.09	5.1	0.17	3.9										
159.25613.963	13.136924	0.18	4.8	0.46	4.2	0.21	1.1								
159.25745.544	9.229714	0.08	0.8	0.18	3.7										
161.25086.954	9.085517	0.20	2.7	0.42	4.5	0.16	3.0	0.14	1.8						
162.25086.6466	9.085511	0.21	4.9	0.40	4.4	0.18	2.2								
162.25343.874	8.986217	0.11	1.1	0.22	4.4										
162.25348.3066	11.706059	0.19	2.5	0.40	4.0	0.17	1.6	0.08	6.2						
162.25475.771	11.272678	0.14	2.4	0.25	4.3										
162.25478.743	9.924855	0.20	4.0	0.43	4.1	0.20	1.8								
162.25996.475	10.801278	0.14	6.2	0.19	4.2										

TABLE 3B

R-BAND FOURIER AMPLITUDE RATIOS AND PHASE DIFFERENCES FOR THE 79 OBJECTS IN OUR SAMPLE OF MACHO DELTA SCUTI STARS HAVING A FIRST FOURIER HARMONIC (A_2). A_{n1} IS THE RATIO OF n-TH TO FUNDAMENTAL FOURIER HARMONIC AMPLITUDES. ϕ_{n1} IS THE NORMALIZED PHASE DIFFERENCE $\phi_n - n\phi 1$ IN RADIANS.

MACHO Star #	ν	A_1	ϕ_1	A_{21}	ϕ_{21}	A_{31}	ϕ_{31}	A_{41}	ϕ_{41}	A_{51}	ϕ_{51}	A_{61}	ϕ_{61}	A_{71}	ϕ_{71}
101.20648.1571	9.766988	0.09	1.7	0.30	3.1										
101.21305.255	8.918816	0.14	3.0	0.43	4.4	0.13	2.1	0.09	6.0						
101.21436.366	6.083023	0.07	4.8	0.14	3.6										
101.21437.1516	9.585009	0.20	5.4	0.43	3.9	0.22	1.6								
101.21821.2017	14.028103	0.21	5.5	0.40	4.2										
102.22591.871	8.863148	0.14	6.0	0.37	5.0										
102.22721.762	10.103451	0.10	0.9	0.34	4.1										
102.23504.1024	10.757620	0.14	3.9	0.43	5.1										
103.24024.815	11.987896	0.10	5.4	0.38	4.1	0.17	1.6								
103.24034.3894	10.686740	0.05	1.5	0.13	4.3										
103.24284.695	10.896136	0.11	3.1	0.26	4.0										
104.19990.4660	10.415403	0.15	2.0	0.24	4.1	0.09	1.5								
104.20130.854	8.037423	0.14	4.8	0.37	4.1										
105.21808.288	8.773583	0.15	0.2	0.40	4.0	0.17	1.7								
105.21947.1957	8.929778	0.13	5.1	0.36	3.7										
109.19721.2119	8.259985	0.13	1.8	0.39	4.0	0.24	1.7								
109.19849.222	5.486534	0.18	4.1	0.47	4.2	0.25	2.4	0.09	6.1	0.04	4.5	0.07	1.3		
109.19990.879	10.415396	0.15	4.6	0.27	4.1										
109.20372.410	7.918786	0.13	1.3	0.27	4.5										
109.20377.3241	8.930567	0.11	2.9	0.36	4.3										
109.20508.1186	7.423864	0.14	4.3	0.45	4.1	0.24	2.1	0.12	6.1						
109.20638.40	8.680859	0.07	5.0	0.15	4.3										
109.20762.936	8.764776	0.09	2.0	0.31	3.4										
109.20890.1400	10.199457	0.22	4.1	0.40	4.2	0.16	2.0	0.10	5.6						
110.22836.520	10.194366	0.11	1.8	0.41	4.2	0.12	2.2								
110.23356.737	9.200613	0.19	0.8	0.41	3.8	0.20	1.4	0.15	5.7	0.07	3.3				
111.23882.712	8.920773	0.14	5.2	0.48	4.2	0.21	2.1								
113.18159.547	5.140253	0.11	5.9	0.42	4.5	0.15	3.1								
113.19324.1134	9.327369	0.15	2.7	0.40	4.0	0.21	1.8								
113.19452.883	8.129420	0.10	1.8	0.30	3.7										
114.19716.1463	8.923152	0.14	6.0	0.33	4.4	0.09	2.2								
114.19840.890	7.963950	0.12	5.1	0.27	3.8										
114.19849.2274	5.486536	0.17	0.2	0.50	4.1	0.23	2.1	0.08	0.3	0.07	3.4	0.12	1.0	0.07	0.1
114.19969.980	9.683205	0.13	2.2	0.23	4.4										
114.20108.1218	10.855722	0.14	3.2	0.34	4.1	0.12	1.9								
114.20230.3899	9.633618	0.11	5.4	0.15	4.9										
114.20368.797	8.552585	0.06	3.1	0.24	4.2										
114.20620.159	7.815573	0.07	0.7	0.10	3.6										
115.23092.1144	10.896281	0.14	5.0	0.45	4.0	0.19	1.9								
115.23344.1034	11.420648	0.23	3.7	0.43	3.8	0.15	1.8	0.16	5.5						
115.23474.197	10.065422	0.17	0.8	0.34	4.1	0.19	1.7	0.12	6.1	0.06	4.6				
116.24123.2368	8.993959	0.12	0.7	0.46	4.1										
116.24124.2364	10.373105	0.20	3.2	0.30	4.5	0.16	2.3								
116.24131.2209	11.768418	0.13	1.8	0.40	3.9										
116.24384.481	11.505569	0.15	4.4	0.31	4.5	0.16	1.6								
118.17885.605	6.415236	0.14	0.8	0.28	4.2										
118.18270.1993	7.594984	0.25	4.4	0.40	4.2	0.19	2.4								
118.18921.1569	9.528644	0.17	4.1	0.31	4.3										
119.19574.1169	9.359298	0.08	1.0	0.23	3.3										
119.19835.439	5.275013	0.13	2.8	0.31	4.4	0.12	2.1								
119.20351.905	6.200649	0.13	2.4	0.31	4.4										
119.20738.147	10.304626	0.06	2.8	0.13	4.0										

TABLE 3B—*Continued*

MACHO Star #	ν	A_1	ϕ_1	A_{21}	ϕ_{21}	A_{31}	ϕ_{31}	A_{41}	ϕ_{41}	A_{51}	ϕ_{51}	A_{61}	ϕ_{61}	A_{71}	ϕ_{71}
119.20738.827	10.388032	0.14	1.3	0.36	4.1	0.15	2.3								
119.20742.2231	9.906815	0.14	6.1	0.42	4.2										
120.21131.780	11.539582	0.10	1.0	0.30	5.1										
120.21396.683	8.845706	0.13	4.3	0.27	5.0										
120.21785.976	9.243728	0.12	0.5	0.26	4.2	0.10	1.1								
121.21388.153	10.070951	0.10	2.1	0.26	3.7										
121.21904.664	10.453621	0.13	0.5	0.30	4.0	0.13	1.6								
121.22291.582	10.361032	0.15	1.2	0.42	4.1	0.15	1.8								
121.22427.551	10.312683	0.16	3.0	0.24	4.0										
124.21891.372	10.525859	0.08	3.8	0.16	4.2										
124.21893.553	9.144923	0.17	6.2	0.38	4.0	0.17	1.9								
124.21894.405	11.248193	0.09	2.9	0.14	3.8										
124.22412.549	11.784227	0.11	1.0	0.32	4.6	0.13	2.1								
125.23847.221	10.766746	0.15	2.7	0.28	4.3										
128.21153.1181	8.849363	0.17	0.1	0.42	4.1	0.19	1.6	0.07	6.2						
128.21405.697	7.896792	0.08	5.2	0.21	4.0										
128.21542.753	10.806030	0.06	2.6	0.25	4.8										
128.21665.609	9.226202	0.07	5.1	0.16	4.4										
159.25613.963	13.136924	0.14	4.8	0.41	4.4	0.18	1.6								
159.25745.544	9.229714	0.06	0.8	0.17	3.9										
161.25086.954	9.085517	0.16	2.7	0.44	4.5	0.17	2.8	0.09	1.8						
162.25086.6466	9.085511	0.15	4.9	0.42	4.4	0.23	2.2								
162.25343.874	8.986217	0.09	1.1	0.20	4.4										
162.25348.3066	11.706059	0.14	2.5	0.37	4.1	0.17	1.8	0.08	0.3						
162.25475.771	11.272678	0.11	2.4	0.24	4.4										
162.25478.743	9.924855	0.16	4.0	0.46	4.3	0.23	2.1								
162.25996.475	10.801278	0.11	6.2	0.15	4.0										

TABLE 4A

THE TEN CONFIRMED DOUBLE- AND MULTIPLE-MODE PULSATORS DETECTED IN THE MACHO CATALOG. PHASES ARE IN RADIANS RELATIVE TO t_0 GIVEN IN TABLE 1. NOTES CONTAIN EITHER THE FREQUENCY RATIO (NUMBER) OR INDICATE THE TYPE OF PULSATION MODE: INTEGER MULTIPLE, SUM, OR POSSIBLE NONRADIAL.

MACHO star	frequency (cycd)	A_V	ϕ_V	A_R	ϕ_R	Notes
104.20389.1202	6.34464	0.057	2.0	0.044	1.9	
	8.45177	0.038	3.9	0.026	3.9	0.75069
109.20634.24	5.61171	0.055	1.9	0.043	1.9	
	5.47079	0.019	2.8	0.014	2.9	nonradial?
	6.92653	0.015	5.5	0.012	5.4	0.81018
	6.85830	0.013	4.6	0.012	4.6	0.81824
109.20638.40	8.68086	0.092	5.0	0.073	5.0	
	17.36172	0.013	5.8	0.011	5.8	$2f_1$
	11.55858	0.013	3.8	0.013	3.8	0.75103
114.19840.890	7.96395	0.143	5.1	0.117	5.1	
	10.33167	0.052	1.4	0.033	1.4	0.77083
	15.92791	0.040	0.1	0.032	0.1	$2f_1$
	18.29552	0.029	1.7	0.023	1.8	$f_1 + f_2$
114.19969.980	9.68320	0.171	2.2	0.133	2.2	
	19.36638	0.039	0.1	0.030	0.1	$2f_1$
	12.52957	0.037	1.2	0.029	1.2	0.77283
114.20368.797	8.55258	0.073	3.1	0.056	3.1	
	10.82242	0.026	6.2	0.021	0.1	0.79027
	17.10518	0.020	2.0	0.014	2.1	$2f_1$
119.19574.1169	9.35930	0.099	1.0	0.080	1.0	
	12.08875	0.087	2.3	0.074	2.4	0.77422
	18.71868	0.025	4.8	0.019	4.9	$2f_1$
	21.44804	0.024	5.3	0.027	5.2	$f_1 + f_2$
121.22427.551	10.31268	0.205	3.0	0.157	3.0	
	23.48304	0.052	3.5	0.034	3.6	$f_1 + f_2$
	13.17041	0.042	5.7	0.030	5.5	0.78302
	20.62532	0.041	2.0	0.038	2.0	$2f_1$
128.21542.753	10.80603	0.077	2.5	0.064	2.6	0.77084
	8.32973	0.051	2.7	0.044	2.9	
	21.61200	0.020	0.3	0.016	0.4	$2f_2$
	19.13576	0.020	1.3	0.018	1.3	$f_1 + f_2$
162.25343.874	8.98622	0.108	1.1	0.086	1.1	
	11.64074	0.041	0.6	0.034	0.6	0.77196
	17.97240	0.024	4.2	0.017	4.2	$2f_1$

TABLE 4B

THE EIGHT CANDIDATE DOUBLE- AND MULTIPLE-MODE PULSATORS DETECTED IN THE MACHO CATALOG. PHASES ARE IN RADIANS RELATIVE TO t_0 GIVEN IN TABLE 1. NOTES CONTAIN EITHER THE FREQUENCY RATIO (NUMBER) OR INDICATE THE TYPE OF PULSATION MODE: INTEGER MULTIPLE, SUM, OR POSSIBLE NONRADIAL.

MACHO star	frequency (cycd)	A_V	ϕ_V	A_R	ϕ_R	Notes
109.20378.2701	9.63835	0.048	3.6	0.038	3.7	nonradial?
	9.65558	0.030	3.4	0.023	3.4	""
	10.13476	0.011	2.8	0.009	2.5	""
114.20108.1218	10.85572	0.179	3.2	0.143	3.2	
	21.71143	0.062	2.3	0.049	2.3	$2f_1$
	32.56717	0.024	1.4	0.018	1.4	$3f_1$
	13.79556	0.013	5.2	0.016	5.4	0.78690
115.22573.263	10.89872	0.185	5.7	0.157	5.7	
	14.11001	0.047	0.8	0.047	0.8	0.77241
116.24384.481	11.50557	0.182	4.4	0.145	4.4	
	23.01107	0.054	4.2	0.044	4.2	$2f_1$
	14.88981	0.029	4.1	0.023	4.1	0.77271
	34.51673	0.025	5.4	0.023	5.3	$3f_1$
119.19835.439	5.27501	0.167	2.8	0.130	2.8	
	10.55000	0.056	1.3	0.040	1.2	$2f_1$
	15.82508	0.022	0.3	0.015	0.1	$3f_1$
	8.67222	0.021	2.2	0.021	2.4	0.60827
	8.61755	0.018	2.7	0.018	2.7	0.61212
120.21785.976	9.24373	0.158	0.5	0.121	0.5	
	18.48747	0.039	3.3	0.031	3.2	$2f_1$
	27.73122	0.014	0.4	0.012	0.6	$3f_1$
	12.98294	0.015	1.5	0.013	1.7	0.71199
162.25475.771	11.27268	0.142	2.4	0.111	2.4	
	14.48269	0.040	0.6	0.031	0.4	0.77836
	22.54535	0.035	0.5	0.027	0.4	$2f_1$
	14.40240	0.028	1.9	0.022	1.7	0.78269
	25.75540	0.019	5.2	0.017	5.7	$f_1 + f_{2a}$
162.25996.475	10.80128	0.136	6.2	0.114	6.2	
	21.60252	0.026	2.0	0.017	2.1	$2f_1$
	10.80047	0.029	0.7	0.028	0.7	nonradial?